の各部位に存在するニューロン集団を個別に狙ってチャネルロドプシン2を発現させ，チャネルロドプシン2を発現していない皮質ニューロンにガラス電極を当て，その周囲に微小なスポットで光刺激を行った．チャネルロドプシン2発現細胞が記録細胞へシナプス結合をしていると電気応答が得られるので，チャネルロドプシン2発現細胞がどの皮質ニューロンと，細胞のどの部位でシナプス結合をしているのかを詳細に調べ，視床後内腹側核の神経線維が皮質第5層のニューロンに投射しているが，細胞体周囲の第5層と，少し離れた第4層領域でシナプスを形成していることを明らかにした（文献10）．

2）視覚機能の回復　中途失明の原因の一つである網膜色素変性は，最も一般的な遺伝的眼疾患の一つである．おもに夜盲症に始まり，しだいに視野狭窄が進行し，ついには失明する．病態の悪化度は疾患により異なるが，共通する病理変化は網膜の外側にある光受容細胞と網膜色素上皮において顕著に見られる．薄暗いところでものを見る際に働く桿体視細胞などの光受容細胞が死滅することにより，視覚機能が失われる．

そこで，網膜に残存する双極細胞や神経節細胞にチャネルロドプシン2を発現させ，光受容細胞の代わりに光情報を受容し，脳の視覚野へ伝達することで視覚機能を再建する試みが世界の三つのグループでほぼ同時にかつ独立に開始された．筆者らのグループ（富田浩史ら，文献8）は，網膜色素変性モデルラットの眼球にアデノ随伴ウイルスベクターを用いてチャネルロドプシン2を導入し，網膜内部表面に存在する神経節細胞に光感受性を与えた．このラットの目に青色LED光照射を行うと，大脳皮質視覚野から光照射に応じて視覚誘発性電位（VEP）が記録された（図5）．これは，チャネルロドプシン2を導入したラットでは，光受容細胞が失われたにもかかわらず，目から入った光情報が脳へと伝達されたことを示している．富田らはさらに，ラットの周囲で縦縞の模様を回転させ，その首振り運動を観察することで，ラットが「見えて」いるかのテストを行った．モデルラットでは，チャネルロドプシン2を導入した場合のみ，回転の方向につられて首を振る行動が観察されたことから，少なくとも縞模様の動きを検知することが可能な程度の視覚機能が回復していることが示唆される．

今後の展望

脳機能の光測定と光制御技術は新たな研究手法として神

経科学の大きな一領域であり，そのポテンシャルは計り知れない．より自然に近い状態で，脳の深部に存在するニューロンの活動を監視し制御するこれらの技術は，脳と身体を含めた統合的なシステムの一素子としてのニューロンやそのネットワークの働きを解明することを可能にする．また，光を用いて，ニューロンネットワークやさらには，脳と双方向通信するブレイン・マシン・インターフェース（BMI）技術が展望され，筆者らのグループも研究に着手している（コラム2参照）．チャネルロドプシンのタンパク質構造と機能メカニズムにはまだまだ不明な点が多く，発色団の光子吸収とそれに伴うタンパク質構造変化とイオン透過機構の解明が待たれる．それには，神経科学だけでなく，光生物学，分子生物学，生物物理学，構造生物学，エレクトロニクスなどを含めた学際的な協力が求められている．

参考文献

1. 石塚 徹，八尾 寛，生物物理，**48**，180（2008）．
2. 石塚 徹，八尾 寛，化学と生物，**43**，245（2005）．
3. G. ミーセンベック，日経サイエンス，**39**，48（2009）．
4. 富田 浩史ほか，臨床眼科，**62**，336（2008）．
5. T. Ishizukaほか，*Neurosci. Res.*，**54**，85（2006）．
6. H. Wangほか，*J. Biol. Chem.*，**284**，5685（2008）．
7. Y. Sugiyamaほか，*Photochem. Photobiol. Sci.*，**8**，328（2009）．
8. H. Tomitaほか，*Invest. Ophthalmol. Vis. Sci.*，**48**，3821（2007）．
9. F. Zhangほか，*Nat. Rev. Neurosci.*，**8**，732（2007）．
10. L. Petreanuほか，*Nature*（London）**457**，1142（2009）．

コラム2　チャネルロドプシンの可能性

●ブレイン・マシン・インターフェース（BMI），ブレイン・コンピューター・インターフェース（BCI）

脳情報を解読し，それを機械の制御やコンピューターへの入力情報に利用するとともに，脳に情報をインプットする技術は，ブレイン・マシン・インターフェース（BMI），ブレイン・コンピューター・インターフェース（BCI）とよばれている．これらは，脳を介した新たなコミュニケーションを可能とする技術であり，その実現のためには，低侵襲で長期安定型の脳情報双方向活用技術の発展が不可欠である．時間・空間的に高密度，高解像度の情報入出力を実現するにあたり，光を双方向的情報媒体として用いることが理想的である．また，光を用いることにより，脳に対する機械的な侵襲を最小限にとどめることができる．チャネルロドプシンは，光を用いた脳への情報入力媒体（フォトバイオ機能モジュール）として理想的である．

●ニューロンネットワークを利用したコンピューター素子の開発

コンピューターは，情報を早く，正確に処理する能力に優れている．また，ネットワークにより，リアルタイムに世界中のコンピューターと交信することができる．これに対して，脳は，エラーを積極的につくりだし，多くの選択肢の中から環境や状況に最適の解答を引き出す能力に優れている．この能力がインスピレーションや感情などの源になっている．そこで，ニューロンネットワークを人工的なハードウェアと組合わせることにより，より脳に近い情報処理のできるコンピューターを作製することが試みられている．

具体的な方法として，シリコン基板やガラス板を加工して，刺激用および測定用の電極をマトリックス上に配置したものに，培養ニューロンや脳スライスをセットしたものが用いられている．また，生きている動物の脳そのものをコンピューターの情報処理に用いる試みもなされている．ニューロンを刺激する方法として，金属や半導体電極による電気刺激法やグルタミン酸投与法が用いられてきた．従来の方法は，空間解像度が低いという問題があった．また，生きている動物を用いる場合，多電極刺激装置などを脳に埋め込む必要があり，侵襲的であり，長期間の安全な使用が難しかった．

しかし，チャネルロドプシンを遺伝子導入し，発現させることにより，神経細胞に光感受性を獲得させることができる．培養ニューロンの場合，レーザーなどを用いることにより，個々のニューロン，さらには，その一部を多点同時刺激することが可能になり，複雑なパターンの情報をニューロンネットワークに送り込むことができる．これにより，単純な培養ニューロンネットワークであっても，脳が行っている試行錯誤的な情報処理を再現することが可能になる．生きている動物の大脳皮質を用いる場合は，脳表面からの光照射により，高い解像度をもって，多点同時のパターン刺激が実現される．光刺激を用いる場合，電気的なアーチファクトが生じないので，同時に個々のニューロンの活動をリアルタイムに計測し，コンピューターにフィードバックすることが容易になる．これにより，従来のコンピューターの能力に，パターン認識，自己組織化など脳の優れた能力をあわせもつコンピューターが作られることが期待される．さらには，コンピューターが人間に近い感情をもつようになるだろう．

〈参考〉特開（A）2006－217866光感受性を新たに賦与した神経細胞　文部科学省「脳科学研究推進プログラム」ホームページ（http://brainprogram.mext.go.jp/）

Experimental Eye Research 90 (2010) 429–436

Contents lists available at ScienceDirect

Experimental Eye Research

journal homepage: www.elsevier.com/locate/yexer

Channelrhodopsin-2 gene transduced into retinal ganglion cells restores functional vision in genetically blind rats☆

Hiroshi Tomita [a,*], Eriko Sugano [a], Hitomi Isago [a,b], Teru Hiroi [a], Zhuo Wang [a], Emi Ohta [a], Makoto Tamai [b]

[a] *Tohoku University, Institute for International Advanced Interdisciplinary Research, 4-1 Seiryo-machi, Aoba-ku, Sendai, 980-8575 Japan*
[b] *Tohoku University Graduate School of Medicine, Japan*

ARTICLE INFO

Article history:
Received 17 July 2009
Accepted in revised form 10 December 2009
Available online 27 December 2009

Keywords:
channelrhodopsin-2
Royal College of Surgeons rat
retinal ganglion cells
photoreceptor degeneration
visually evoked potential
retinitis pigmentosa
adeno-associated virus vector

ABSTRACT

To test the hypothesis that transduction of the channelrhodopsin-2 (*ChR2*) gene, a microbial-type rhodopsin gene, into retinal ganglion cells of genetically blind rats will restore functional vision, we recorded visually evoked potentials and tested the experimental rats for the presence of optomotor responses. The N-terminal fragment of the *ChR2* gene was fused to the fluorescent protein Venus and inserted into an adeno-associated virus to make AAV2-ChR2V. AAV2-ChR2V was injected intravitreally into the eyes of 6-month-old dystrophic RCS (rdy/rdy) rats. Visual function was evaluated six weeks after the injection by recording visually evoked potentials (VEPs) and testing optomotor responses. The expression of *ChR2V* in the retina was investigated histologically. We found that VEPs could not be recorded from 6-month-old dystrophic RCS rats that had not been injected with AAV2-ChR2V. In contrast, VEPs were elicited from RCS rats six weeks after injection with AAV2-ChR2V. The VEPs were recorded at stimulation rates <20 Hz, which was the same as that of normal rats. Optomotor responses were also significantly better after the AAV2-ChR2V injection. Expression of ChR2V was observed mainly in the retinal ganglion cells. These findings demonstrate that visual function can be restored in blind rats by transducing the *ChR2V* gene into retinal ganglion cells.

1. Introduction

Channelrhodopsin-2 (ChR2), cloned from the green algae *Chlamydomonas reinhardtii*, is classified as a microbial-type rhodopsin that can be activated by specific wavelengths of light (Nagel et al., 2003; Sineshchekov et al., 2002; Suzuki et al., 2003). ChR2 is similar to bacteriorhodopsin (Oesterhelt and Stoeckenius, 1973), which uses an attached chromophore to absorb photons. A reversible photoisomerization of the all-trans isoform of retinaldehyde changes its conformation, and this directly induces ion movement through the membrane (Oesterhelt, 1998). It is this specific feature that allows ChR2 to function as a cation channel after exposure to light (Nagel et al., 2003).

Retinitis pigmentosa (RP) is a retinal degenerative disease that is associated with a progressive loss of photoreceptor cells resulting in a loss of peripheral visual fields, then central vision, and finally blindness. Mutations of a number of genes have been shown to cause RP, and these genes are mainly related to the phototransduction pathway (RetNet; http://www.sph.uth.tmc.edu/Retnet/). Unfortunately, these findings have not led to a successful way to treat or prevent RP. A new strategy for restoring vision has been recently investigated, viz., transduction of the *channelrhodopsin-2* (*ChR2*) gene into genetically blind mice (Bi et al., 2006). These experiments have been performed on animals that have the same mutation as humans with retinitis pigmentosa (Bowes et al., 1990; Pittler and Baehr, 1991). We have also reported that the intravitreal injection of the *ChR2* gene into older dystrophic Royal College of Surgeons (RCS) rats (Mullen and LaVail, 1976), an animal model of recessively inherited retinitis pigmentosa (D'Cruz et al., 2000; Gal et al., 2000), restored functional vision (Tomita et al., 2007). These observations suggested that transduction of the *ChR2* gene would provide a new method for treating eyes with RP that is independent of the etiology of the retinal degeneration.

Flannery and Greenberg (2006) reported that behavioral testing would be necessary to determine if the use of *ChR2* was a viable

☆ Grant Information: This work was supported in part by Grants-in-Aid for Scientific Research from the Ministry of Education Science and Culture (No. 20791241, 21791664, 21200022), Ministry of Health, Labor and Welfare, Comprehensive Support Programs for Creation of Regional Innovation Science and Technology Incubation Program of the Japanese Government, Japanese Retinitis Pigmentosa Society, and Sumitomo Foundation.

* Corresponding author. Tel./fax: +81 22 717 8207.
E-mail address: hiroshi-tomita@iiare.tohoku.ac.jp (H. Tomita).

0014-4835/$ – see front matter © 2009 Elsevier Ltd. All rights reserved.
doi:10.1016/j.exer.2009.12.006

strategy for restoring functional vision to blind animals. Lagali et al. (2008) reported that ON-bipolar cells that were engineered to be photosensitive by the transfer of the ChR2 gene restored behavioral responses to genetically blind mice. When the *ChR2* gene was transduced into ON-bipolar cells, the retinal ON pathway was selectively activated by light. This is a reasonable way of activating the normal retinal ON pathway, although some methodological difficulties are still present when clinical applications are considered, e.g., the mechanism of gene transfer into ON-bipolar cells. Retinal ganglion cells are good candidates for receiving the ChR2 gene because target genes can be easily transduced into them. We have shown that a single injection of an AAV vector including ChR2 made it possible to change about 30% of all retinal ganglion cells to photosensitive ganglion cells. Recently it was reported that the ectopic expression of melanopsin in the retinal ganglion cells of retinal degeneration mice results in functional vision (Lin et al., 2008). In the same way, it is important to determine whether the ChR2 gene can restore functional vision when transferred retinal ganglion cells.

Thus, the purpose of this study was to determine whether transduction of the *ChR2* gene into retinal ganglion cells of blind RCS rats can restore functional vision. We used visually evoked responses and optomotor responses to assess the functional condition of the visual system. We found that AAV2-mediated *ChR2* transfer can lead to recovery of not only electrophysiological but also optokinetic responses.

2. Materials and methods

The procedures used on the animals in these experiments were in accordance with the ARVO Statement for the Use of Animals in Ophthalmic and Vision Research and the Guidelines for Animal Experiments of Tohoku University.

2.1. Experimental animals

The experiments were conducted on 6-month-old male RCS rats; 18 dystrophic (rdy/rdy), and 4 non-dystrophic (+/+). The rats were obtained from CLEA Japan, Inc. (Tokyo, Japan).

2.2. Vector construction

The construction of the vector expressing ChR2 and the preparation of the vector for injection have been described in detail (Sugano et al., 2005; Tomita et al., 2007). In brief, the N-terminal fragment (residues 1-315; GenBank Accession No. AF461397) of the *ChR2* gene was fused to a fluorescent protein, Venus, in frame at the end of the *ChR2* coding fragment. Then ChR2-Venus (ChR2V) was introduced into the EcoRI and Hind III sites of the 6P1 plasmid (Kugler et al., 2003). The synapsin promoter was exchanged for a hybrid CMV enhancer/chicken β-actin promoter (CAG) (Niwa et al., 1991). The AAV2-ChR2V vector was purified by a single-step column purification method of Auricchio et al. (Auricchio et al., 2001; Sugano et al., 2005).

2.3. AAV vector injection

The method used to inject the AAV-ChR2V vector into the vitreous of both eyes of 6-month-old RCS (rdy/rdy) rats has been described in detail (Tomita et al., 1999, 2007). In brief, rats were anesthetized by an intramuscular injection of a mixture of ketamine (66 mg/ml) and xylazine (33 mg/kg). Under an operating microscope, a small incision was made in the conjunctiva to expose the sclera, and 5 μl of a viral vector suspension at a concentration of $1–10 \times 10^{12}$ genomic particles/ml was injected into the center of the vitreous cavity through the ora serrata with a 32 gauge needle on a 10 μl Hamilton syringe (Hamilton Company, Reno, NV).

2.4. Recording visually evoked potentials (VEPs)

VEPs were recorded before and at one week after the injection of AAV-ChR2V vector with a Neuropack system (MEB-9102; Nihon Kohden, Tokyo, Japan) as described in detail (Tomita et al., 2007). The method of recording was derived from a combination of the protocols used by Papathanasiou et al. (2006) and Iwamura et al. (2003). Briefly, at least seven days before the recordings, silver–silver chloride electrodes were implanted epidurally 7 mm behind the bregma and 3 mm lateral to the midline of both hemispheres. A reference electrode was implanted epidurally on the midline 12 mm posterior to the bregma.

Under ketamine–xylazine anesthesia, the eye was stimulated with 20 ms duration 0.5 Hz photic stimuli. The photic stimuli were generated by pulse activation of a blue light-emitting diode (LED) with light-emitting wavelengths of 435–500 nm (peak at 470 nm). A white LED was used to determine the spectral responsiveness (white LEDs include all wavelengths). The high and low band-pass filters of the amplifier were set to 50 kHz and 0.05 kHz, respectively. One hundred consecutive responses were averaged for each VEP. We also investigated the changes of the VEP responses elicited by a train of stimulus frequencies of 1–50 Hz with a pulse duration of 10 ms.

The stimulus light intensity was measured by a laser power meter (Lasercheck, Edomond Optics, Japan).

2.5. Spectral responsivity of eye after transduction of ChR2V

To investigate the spectral responsivity of the retinas transduced with *ChR2V*, VEPs were elicited by different wavelength stimuli of 1 mW/cm^2. The wavelengths were isolated by band-pass filters (FUJIFILM Japan, Tokyo, Japan; Fig. 1A).

2.6. Behavioral assessments

The behavioral assessments were performed in a head-tracking instrument (Hayashi Seisakusyo, Kyoto, Japan). The instrument consisted of a circular drum rotating around the animal (Cowey and Franzini, 1979; Haruta et al., 2004; Lund et al., 2001). We covered the circular rotating drum with a transparent blue filter (Ultra color filter #67, Toshiba, Japan; filter transmits wavelengths <560 nm) because of the spectral absorption of ChR2. The vertical blue and black stripes subtended an angle of 10°, and the rotation speed was changed from 0 to 0.5, 2, 4, and 8 rpm. The spatial frequency corresponds to 0.05 cycle/degree, but the stimulus spatial frequency will change slightly with rat head position because the animal can freely move on the platform. The luminosity at the center of the holding chamber was set to 500 (1 mW/cm^2), 300 (0.55 mW/cm^2), and 100 lux (0.19 mW/cm^2). Dystrophic and control RCS rats were tested for 4 min at each speed before and after the ChR2 gene transfer.

The head movements of the animals were recorded by a video camera mounted above the apparatus. All movements were recorded at a rate of 29.95 frames/s. The number of movements was analyzed with movement-sensitive software (Move-tr/2D ver.7.0, Library, Tokyo). We made three marks; on the nose, the neck, and the waist of the rat on the software. The marked points were selected in the area that had a distinct color contrast to make it easy to trace them automatically. The software produced the angle of the three marked points. All of the angular movements >5° were considered to be tracking movements if the direction corresponded with the movement of the rotating stimulus. Large movements

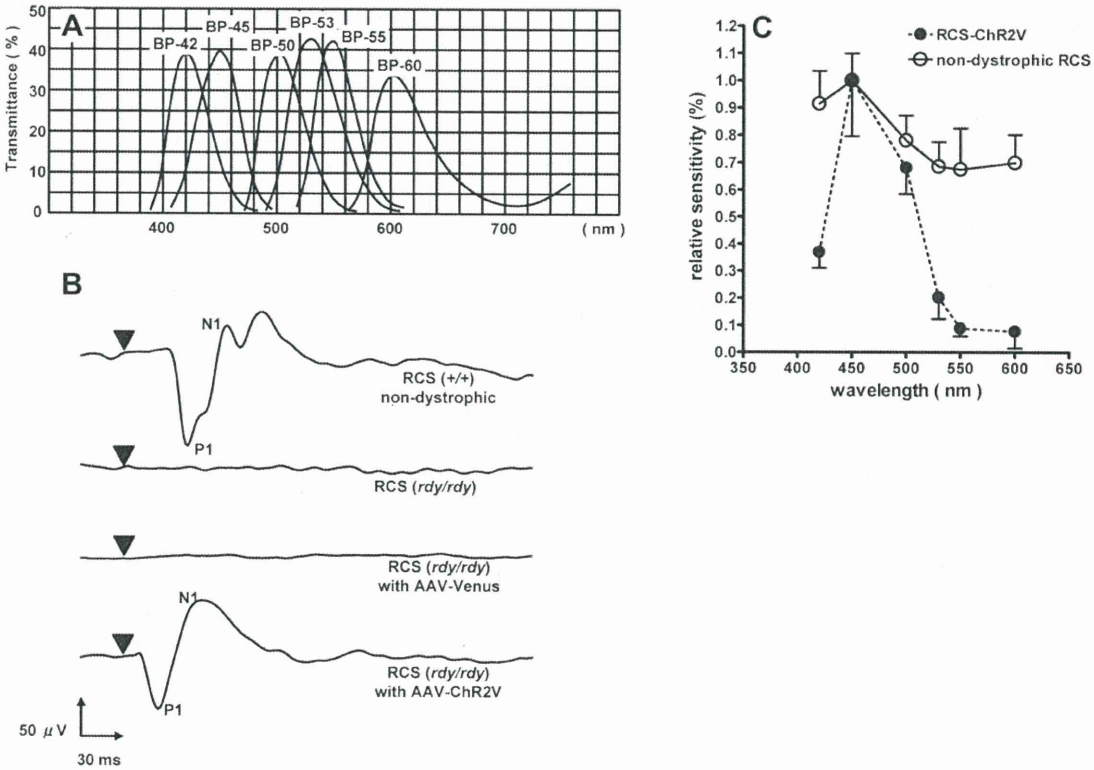

Fig. 1. Spectral responsivity of RCS rats transduced with the *ChR2V* gene. Different parts of the spectrum were isolated by six band-pass filters. A. Band passes for the six band-pass filters used to isolate different wavelengths of the visible spectrum. B. Typical waveforms of the VEPs elicited by 3500 lux stimuli emitted by blue LEDs (435–500 nm, peak at 470 nm). Upper: VEPs from a non-dystrophic rat; VEPs from a dystrophic rat without *ChR2V*; VEPs from a dystrophic rat with *Venus*. Lower: from a dystrophic rat with the *ChR2V* gene. C. Spectral responsiveness of eyes after transduction of *ChR2V* and of eyes of non-dystrophic rats. Amplitudes of VEPs elicited at the different wavelengths at the intensity of 1 mW/cm^2. The relative responses to the amplitude of the stimuli with a 450 nm band-pass filter were plotted. VEPs were recorded by stimuli delivered through each band-pass filter (open circles): non-dystrophic RCS rats ($n = 4$), (closed circles): dystrophic RCS rats with ChR2V ($n = 8$). Error bars represent standard deviations.

with movements of the body of the animal were not counted. The number of movements at 0 rpm was subtracted from that at each rotation speed.

2.7. Retrograde labeling of retinal ganglion cells (RGCs) with fluorogold

To identify the RGCs in the ganglion cell layer (GCL), the RGCs were retrogradely labeled seven days before the rats were sacrificed. The labeling was done by injecting 4 μl of 2% aqueous fluorogold (FG; Fluorochrome, Englewood, CO; Brecha and Weigmann, 1994) containing 1% dimethylsulfoxide into the superior colliculus with a 32 G needle on a Hamilton syringe.

2.8. ChR2V expression in retina

Sixteen weeks after the injection of AAV-ChR2V, rats ($n = 4$) were sacrificed and the eyes were removed and fixed in 4% paraformaldehyde in 0.1 M phosphate buffer. The ipsilateral retinas were isolated and flat-mounted on microscope slides. The fluorogold-labeled and ChR2-expressing cells were counted in 12 distinct areas of the retina (three areas in each quadrant starting 1 mm from the optic nerve) to evaluate the transduction efficiency. Two of the contralateral eyes were embedded in OCT compound (Sakura, Tokyo, Japan) after immersion in 30% sucrose solution in PBS. Fifteen micrometer retinal sections were cut and mounted on slides. The slides of retinal whole mounts and sections were covered with Vectashield medium (Vector Laboratories, Burlingame, CA). The Venus fluorescence was examined with a fluorescence microscope, Axiovert40 (Carl Zeiss).

2.9. Histological studies of the retina

Another two of the eyes were used for paraffin-embedded sections to examine histological changes induced by the expression of ChR2. Analyses of the retinal morphologies in ChR2V−/− and ChR2V+/− rats were performed as described Li et al. (2007). In brief, rats were sacrificed by asphyxiation with carbon dioxide after the induction of photoreceptor degeneration. The eyes were enucleated, fixed, and embedded in paraffin. Three-micrometer thick sections of retinas were cut along the vertical meridian and stained with hematoxylin and eosin to allow examination of the retina in the superior and inferior hemispheres (LaVail et al., 1992).

2.10. Statistical analyses

Statistical analyses was performed using GraphPad Prism software (GraphPad Software, San Diego, CA). The criterion for statistical significance was $P < 0.05$.

3. Results

3.1. Spectral responsivity of ChR2V-expressing retinas

To investigate the spectral responsivity of ChR2V-expressing retinas, visually evoked potentials were elicited by light filtered

through six band-pass filters that isolated different parts of the spectrum (Fig. 1A). Typical waveforms elicited by light filtered through the BP-450 nm filter in rats with or without ChR2V are shown in Fig. 1B. Large amplitude VEPs were recorded from 6-month-old non-dystrophic RCS rats, but no response was elicited from untreated 6-month-old dystrophic RCS rats (Fig. 1B). However, six weeks after the injection of AAV-ChR2V, large (123.0 ± 13.5 μV) VEPs were recorded when the eye was stimulated with a stimulus intensity of 3500 lux (Fig. 1B). The largest amplitude was elicited by the wavelength of 450 nm (Fig. 1C), and VEPs were evoked by stimuli whose wavelengths were ≤550 nm.

3.2. Changes in VEP amplitude at different times after injection of AAV2-ChR2V

VEPs in RCS rats injected with AAV2-ChR2V were first detected two weeks after the injection (Fig. 2A). Thereafter, the amplitude progressively increased up to five weeks post-injection when the mean amplitude was 118.4 μV (Fig. 2A). In dystrophic RCS rats of the same age, VEPs were not detected with the same stimuli (noise level 5 μV). With increasing stimulus intensities, the amplitudes of the VEPs increased and the latencies of P1 decreased (Fig. 2B). Interestingly, the latencies of P1 in the *ChR2*-transduced RCS rats (24.68 ± 2.78 ms) were shorter than those in non-dystrophic RCS rats (49.43 ± 1.21 ms; $P < 0.0001$; un-paired t test; Fig. 2C).

3.3. Changes of VEPs responses by different frequencies of light stimulation

VEPs elicited by different frequencies of light stimulation were recorded from wild-type and dystrophic rats transduced with the *ChR2V* gene. VEPs were recorded from both types of rats when the stimulus frequencies were <20 Hz (Fig. 3A). Responses could not be detected in either type of rat when the stimulus frequencies were 40 Hz and 50 Hz. The responses from both rats were well fit by the Boltzmann fitting curve (Fig. 3B). The amplitudes of the VEPs in rats with *ChR2V* were not affected by a 200 ms interval of a train of light stimuli (Fig. 3C). These results indicated that the responsivity to light allowed by the transduction of *ChR2V* is similar to that in wild-type rats.

3.4. Behavioral assessment by optomotor responses

To determine whether transduction of the *ChR2* gene restored functional vision, optomotor responses were recorded from non-dystrophic normal (Fig. 4A), dystrophic (Fig. 4B) and *ChR2*-transduced RCS rats (Fig. 4C). Preliminary experiments showed that when the angle of the neck moved over 5°, the movements were well correlated with the rotation speed in the non-dystrophic RCS (+/+) rats (Fig. 4D). Therefore, we counted the number of neck movements over 5°. The score in 30-week-old uninjected dystrophic rats at 2 rpm was 3.00 ± 3.64, while that in 30-week-old rats six weeks post-injection was significantly higher 13.31 ± 5.82 ($P < 0.0006$; Fig. 4E). Although non-dystrophic rats (+/+) responded to the rotation even at speeds of 2 rpm at 300 lux and to 4 rpm at 100 lux (Fig. 4F), the rats with the transduced *ChR2V* gene did not respond to the lower light intensities (Fig. 4G).

3.5. ChR2V expression in retina

Histological examination of flat mounts of the retina showed cells over a wide area of the retina had been retrogradely labeled

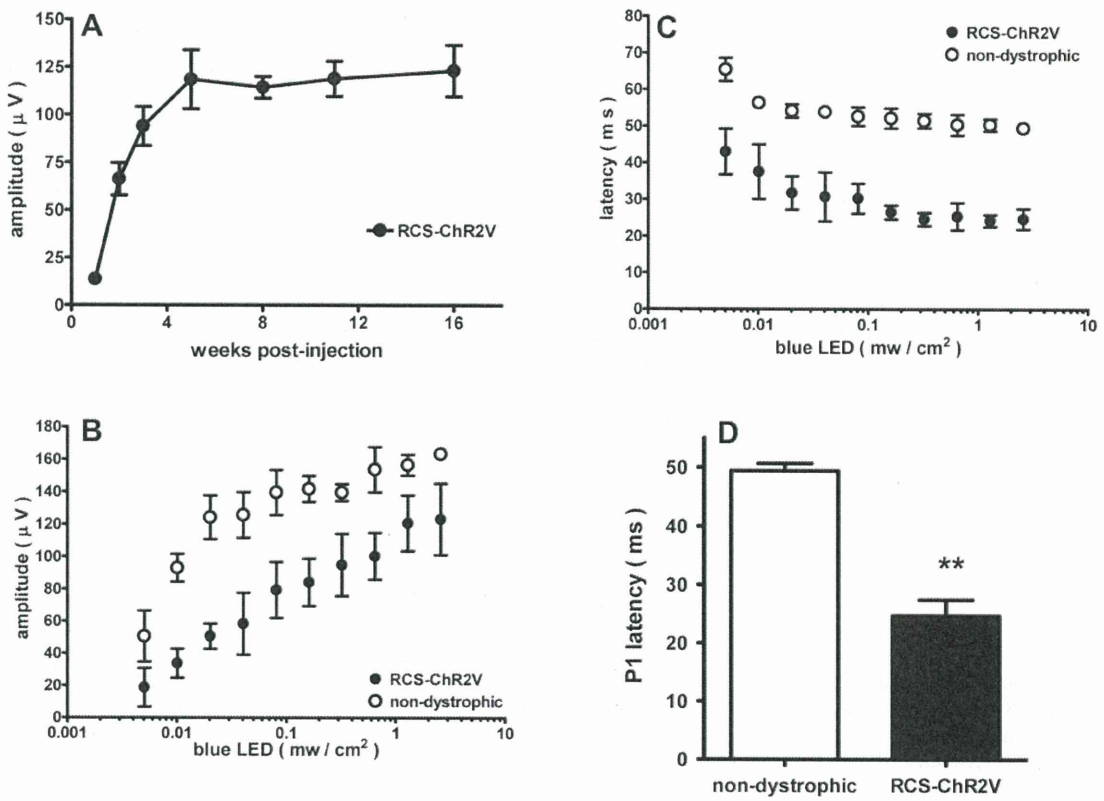

Fig. 2. VEPs recorded from RCS rats transduced with the *ChR2V* gene. A. Changes in amplitude at different weeks after the injection of AAV-ChR2V. B. Changes in amplitude (P1–N1) and latency (P1) elicited by different stimulus intensities. Blue LEDs (435–500 nm, Peak at 470 nm) were used to elicit the VEPs. C. Differences of the P1 latency between non-dystrophic and ChR2V-transduced dystrophic rats. Error bars represent the standard deviation of the mean. The statistical evaluation was performed using the un-paired t test (dystrophic RCS with ChR2V; $n = 8$, non-dystrophic RCS; $n = 4$, $^{**}P < 0.0001$).

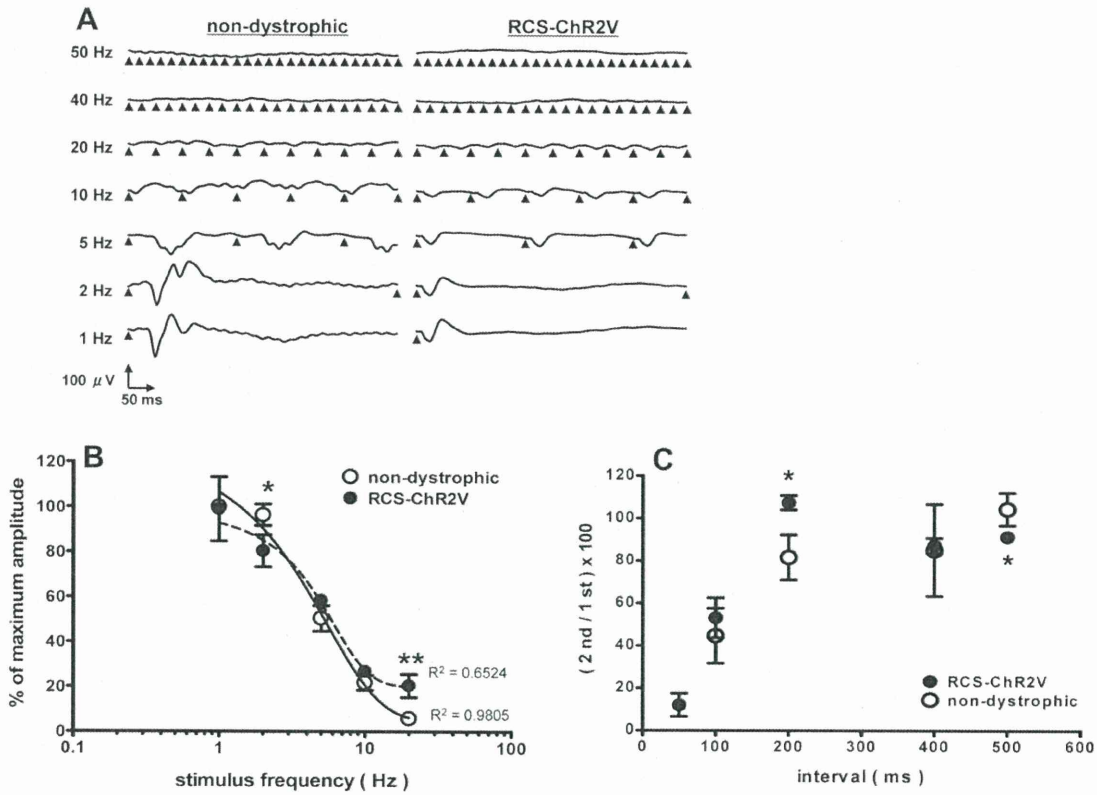

Fig. 3. Changes of responsivity in VEPs elicited by different stimulus frequencies. A. Typical VEP waveforms elicited by different stimulus frequencies. B. Changes in VEP amplitude elicited by different stimulus frequencies. Data are expressed as percentages of the amplitude at 1 Hz. The amplitude recruitment curve was fitted to the Boltzmann model. C. Changes in VEP amplitude elicited by different stimulus trains. Data are expressed as a percentage of the amplitude elicited by the first stimulus. Photic stimuli were generated by a blue LED (435–500 nm, peak at 470 nm) at 3500 lux. The statistical evaluation was performed using the un-paired *t* test (dystrophic RCS with ChR2V; $n = 8$, non-dystrophic RCS; $n = 4$, $^{*}P < 0.05$, $^{**}P < 0.01$).

with Fluorogold (Fig. 5A). These cells were considered to be RGCs (Fig. 5B). Merged images showed that the expression of *ChR2V* was mainly in the RGCs (Fig. 5C). When the AAV-Venus vector was injected, Venus fluorescence was also observed in the RGCs, but the Venus protein was localized in the cell body, which was completely different from those injected with AAV-ChR2V (Fig. 5D). Cryosections showed that the labeled cells were observed in the ganglion cell layer (Fig. 5E and F) and some of them were in the inner nuclear layer (Fig. 5F). Photoreceptor cells were not seen in the retinas of the RCS rats (Fig. 5G). The number of fluorogold-labeled cells, which are most likely retinal ganglion cells, was 2531.8 ± 214.8. The number of double-labeled cells was 710.6 ± 117.7. Thus, the transduction efficiency was about 28.3% (Fig. 5H). Paraffin sections also showed no difference in the thickness of the photoreceptor layer between non-injected and AAV-ChR2-injected retinas (Fig. 5I and J).

4. Discussion

Our results demonstrated that VEPs can be recorded from genetically blind RCS rats that expressed the *ChR2* gene, and the maximum response was elicited by stimuli with a peak wavelength at 450 nm. This agrees with an earlier report that the peak spectral absorption of *ChR2* is approximately at 460 nm (Nagel et al., 2003). In addition, VEPs were elicited by stimuli up to 550 nm, whereas non-dystrophic RCS rats responded to wavelengths over 600 nm. This ability of normal rats to respond to longer wavelengths is probably because they have two cone photopigments with peak absorbances at 359 nm (Deegan and Jacobs, 1993; Yokoyama et al., 1998) and at 510 nm (Neitz and Jacobs, 1986). Therefore, the spectral responsivity spectrum of rats transduced with the *ChR2* gene is somewhat narrower than that of non-dystrophic rats, and this is due to the presence of only channelrhodopsin-2 in the retina.

Distinct VEPs were first recorded at two weeks post-injection. The amplitudes of the VEPs of dystrophic RCS rats carrying the *ChR2* gene in their RGCs gradually increased up to six weeks post-injection. Interestingly, the implicit times (ITs) of the VEPs were shorter than those of non-dystrophic rats. The cause of the shorter ITs was most likely because the neural signals were transduced in the RGCs, and the signals did not have to pass through the inner retinal network. These results suggest that the retinal ganglion cells became photosensitive by the expression of the *ChR2* gene, and the signals generated in the ganglion cells were transmitted to the visual cortex from the RGCs.

We compared the responsivity to different frequencies of light stimulation between non-dystrophic RCS rats and ChR2V-injected rats. The RCS rat with the *ChR2* gene responded up to 20 Hz, which was same as that from non-dystrophic RCS rat. Jehle et al. (2008) reported that steady-state VEPs could elicited by a stimulus frequency of 38 Hz and distinct amplitudes were observed at 19 Hz. The responsivity was slightly higher than our results (20 Hz). The maximum amplitude evoked from RCS rats with *ChR2* was about 50% of that from non-dystrophic RCS rats at 1 Hz. The lower amplitude from rats with ChR2V was probably due to the gene transduction efficiency in the retinal ganglion, which was about 30% of the retinal ganglion cells in this study. We previously

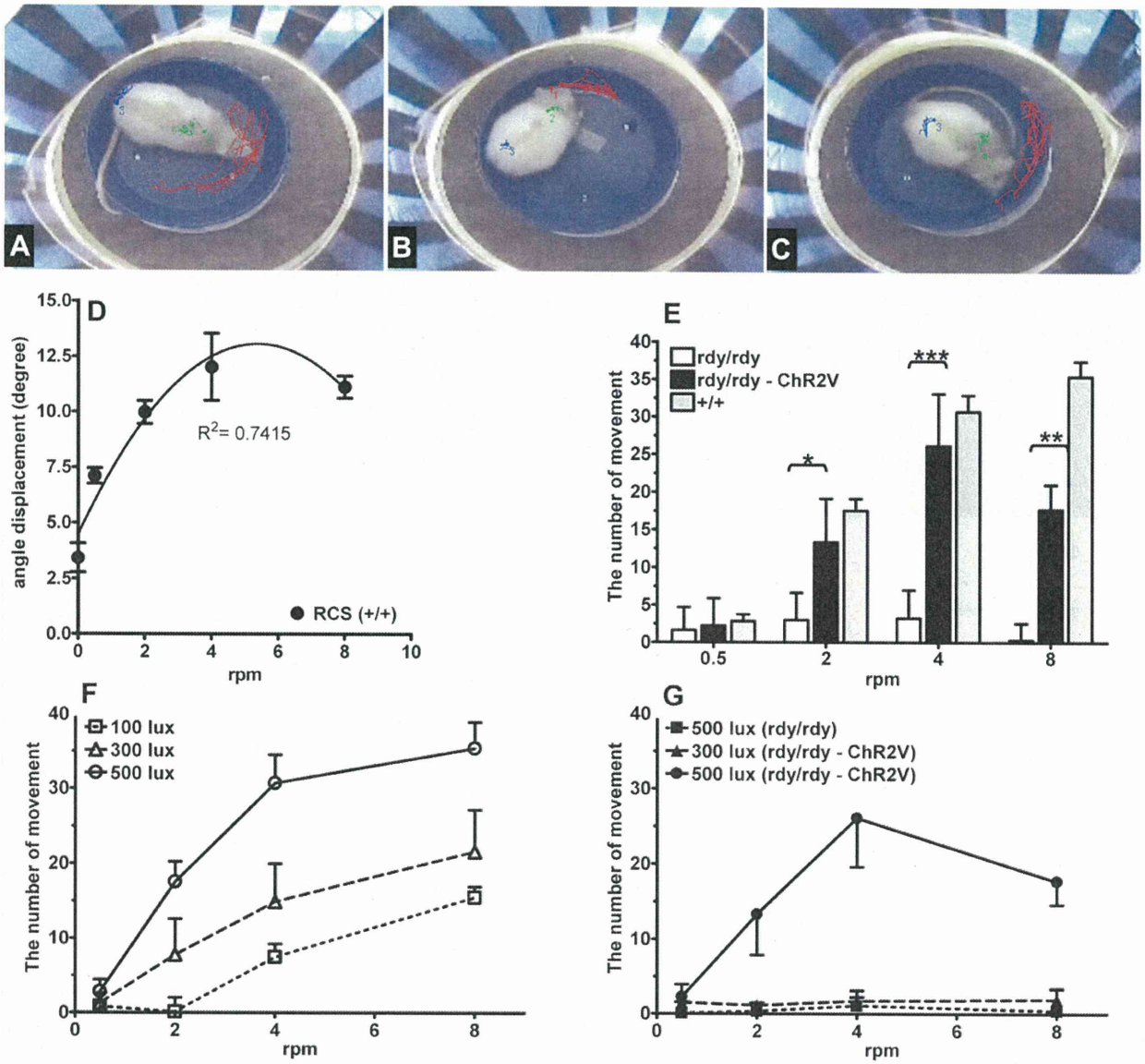

Fig. 4. Behavioral assessment of dystrophic RCS rats and *ChR2V*-transduced rats. The traces of each marked point in non-dystrophic (A), dystrophic (B) and ChR2V-transduced dystrophic (C) rats during a test at 4 rpm. The red, green and blue lines correspond to the marks on the nose, the neck and the waist, respectively. Each score was calculated by subtracting the number of movements at 0 rpm. The angular displacement of each movement in the non-dystrophic rats (D). The luminosity at the center of the holding chamber was set to 500 lux (E). Effects of light intensity on the movements of non-dystrophic (F) and dystrophic RCS rats with ChR2V (G). The score of the non-dystrophic rats increased with increasing light intensities. The drum with black and transparent blue stripes was rotated at speeds of 0, 0.5, 2, 4 and 8 rpm. Error bars represent standard deviations of the means (un-paired t test; $n = 8$, $^{*}P < 0.05$, $^{**}P < 0.01$, $^{***}P < 0.001$).

reported that the transduction efficiency of 10-month-old RCS rats was about 30% (Tomita et al., 2007). The transduction efficiency in the 6-month old rats we used in this study was approximately the same. The AAV we used in this study required host-cell synthesis of the complementary strand for transduction. The failure to undergo viral second-strand synthesis leads to a lower efficiency of transgene expression (Ferrari et al., 1996; Fisher et al., 1996). The use of self-complementary AAV (scAAV) vectors that do not require synthesis of the complementary strand for transgene expression can circumvent this problem. Thus, this method has the possibility of being more efficient and acting more rapidly (Andino et al., 2007; Jayandharan et al., 2008; McCarty et al., 2001).

To determine the functional visual capabilities of *ChR2*-transduced RCS rats, we investigated their optomotor responses (Haruta et al., 2004; Lund et al., 2001). The a-wave of the ERG is an indicator of photoreceptor function, and it disappears by 80–100 days in dystrophic RCS rats (Bush et al., 1995; Sauve et al., 2004). However, the activity of single ganglion cells could be recorded from the optic tract of RCS rats even after the electroretinogram (ERG) could not be recorded (Cicerone et al., 1979). Assessments of their visual sensitivity as determined by electric potentials recorded from the superior colliculus indicated that the sensitivity progressively decreased to reach a plateau at 180–240 days (Sauve et al., 2001). Therefore, we chose 8-month-old RCS rats (2 months after the injection of AAV-ChR2V) for the behavioral assessments. The behavioral scores of the ChR2-transduced RCS rats were significantly higher than those of untreated rats. We also found that the scores of the ChR2-transduced RCS rats were affected by the light intensity in the drum (Fig. 4F).

Lagali et al. (2008) reported that ON-bipolar cells that were engineered to be photosensitive by the transduction of the ChR2

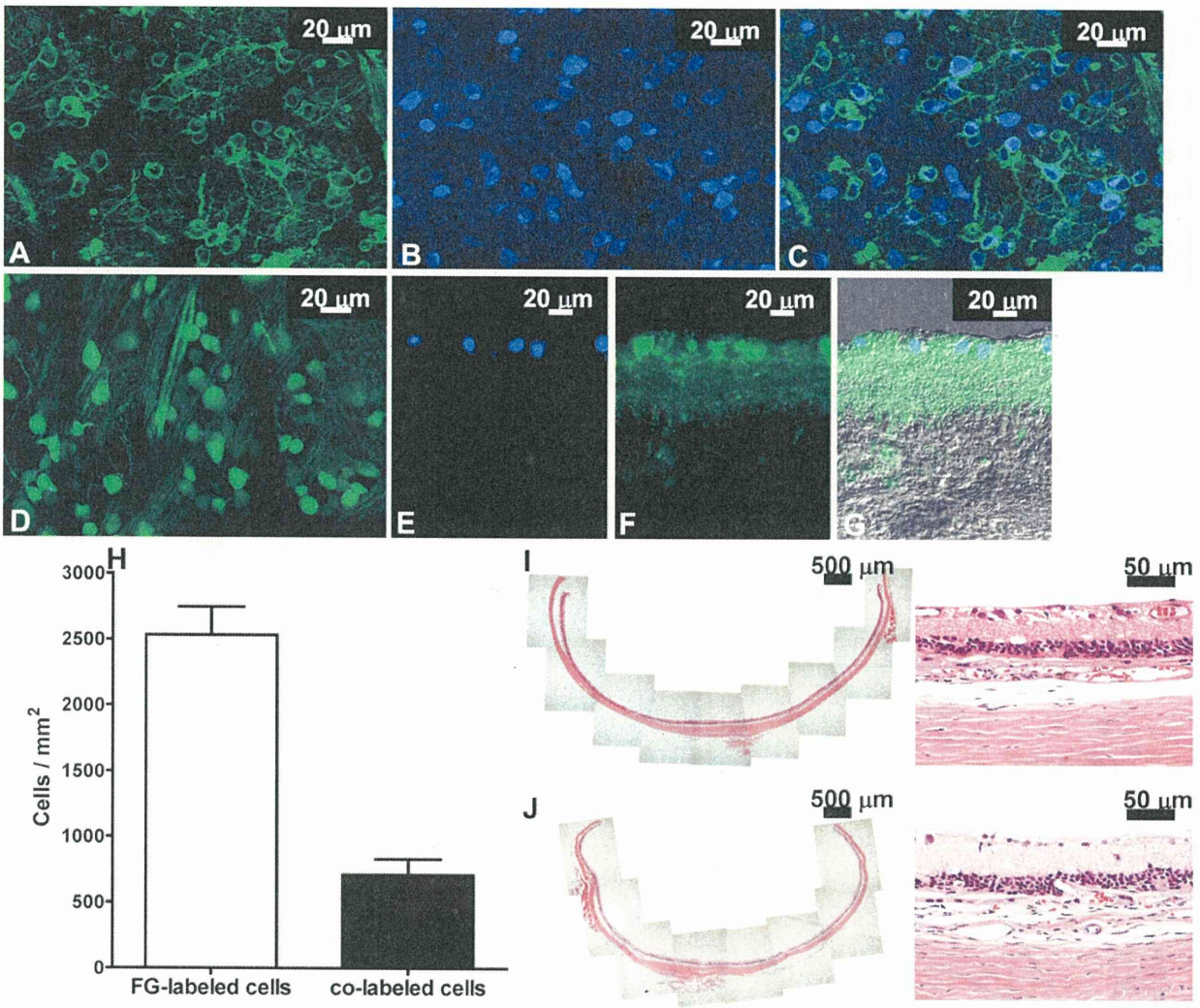

Fig. 5. Expression of ChR2V in the retina. Histological examination of retinas of rats injected with AAV-ChR2V at 16 weeks after the injection. A. Flat-mounted section showing the expression of *ChR2V* gene by green fluorescence. B. Retinal ganglion cells that were retrogradely labeled with fluorogold. C. Merged photograph showing both fluorogold and ChR2V. Many cells are double-labeled. D. Flat-mounted section from a rat transduced with AAV-Venus as a control vector. E. Merged photograph of the Nomarski image, Fluorogold (F) and ChR2V (G). H. The transduction efficiency of ChR2 gene into RGCs ($n = 8$). Hematoxilin–eosin sections from both non-injected RCS rats (I) and AAV-ChR2V-injected RCS rats (J) revealed a loss of photoreceptors in the entire retina.

gene restored visual function to eyes with retinal degeneration. ON and OFF bipolar cells receive synaptic input from photoreceptors. The ON-bipolar cells are one of the candidate cells for receipt of the ChR2 gene because ChR2 can elicit light-on responses. However, some reports have been published that retinal remodeling is triggered in bipolar cells and horizontal cells following photoreceptor degeneration (Marc et al., 2003, 2007; Strettoi and Pignatelli, 2000; Strettoi et al., 2002, 2003). Therefore, the function of the inner retinal layers, including the ON-bipolar pathway, might have some differences from that in normal eyes.

We found that behavioral responses could not be elicited by stimulus intensities <300 lux, although rats could respond at 500 lux. The 500 and 300 lux intensities correspond to about 2.25×10^{15} and 1.24×10^{15} photon/cm^2, respectively. The critical light intensity that elicited behavioral responses in rats with ChR2 transduced into their RGCs was expected to be 2.25×10^{15} photon/cm^2 s, which was close to the light level (3×10^{15} photon/cm^2 s) (Lagali et al., 2008) reported in the behavioral experiments performed on mice with ChR2 transduced into their ON-bipolar cells.

Our findings that ChR2 transduced-ganglion cells could restore visual function both electrophysiologically and behaviorally demonstrate that ganglion cells should also be considered as promising candidates cells for restoring vision via transfer of the ChR2 gene.

Acknowledgements

We thank Prof. Duco Hamasaki for discussions and editing the manuscript.

References

Andino, L.M., Conlon, T.J., Porvasnik, S.L., Boye, S.L., Hauswirth, W.W., Lewin, A.S., 2007. Rapid, widespread transduction of the murine myocardium using self-complementary Adeno-associated virus. Genet. Vaccines Ther. 5, 13.

Auricchio, A., Hildinger, M., O'Connor, E., Gao, G.P., Wilson, J.M., 2001. Isolation of highly infectious and pure adeno-associated virus type 2 vectors with a single-step gravity-flow column. Hum. Gene Ther. 12, 71–76.

Bi, A., Cui, J., Ma, Y.P., Olshevskaya, E., Pu, M., Dizhoor, A.M., Pan, Z.H., 2006. Ectopic expression of a microbial-type rhodopsin restores visual responses in mice with photoreceptor degeneration. Neuron 50, 23–33.
Bowes, C., Li, T., Danciger, M., Baxter, L.C., Applebury, M.L., Farber, D.B., 1990. Retinal degeneration in the rd mouse is caused by a defect in the beta subunit of rod cGMP-phosphodiesterase. Nature 347, 677–680.
Brecha, N.C., Weigmann, C., 1994. Expression of GAT-1, a high-affinity gamma-aminobutyric acid plasma membrane transporter in the rat retina. J. Comp. Neurol. 345, 602–611.
Bush, R.A., Hawks, K.W., Sieving, P.A., 1995. Preservation of inner retinal responses in the aged Royal College of Surgeons rat. Evidence against glutamate excitotoxicity in photoreceptor degeneration. Invest. Ophthalmol. Vis. Sci. 36, 2054–2062.
Cicerone, C.M., Green, D.G., Fisher, L.J., 1979. Cone inputs to ganglion cells in hereditary retinal degeneration. Science 203, 1113–1115.
Cowey, A., Franzini, C., 1979. The retinal origin of uncrossed optic nerve fibres in rats and their role in visual discrimination. Exp. Brain Res. 35, 443–455.
D'Cruz, P.M., Yasumura, D., Weir, J., Matthes, M.T., Abderrahim, H., LaVail, M.M., Vollrath, D., 2000. Mutation of the receptor tyrosine kinase gene Mertk in the retinal dystrophic RCS rat. Hum. Mol. Genet. 9, 645–651.
Deegan 2nd, J.F., Jacobs, G.H., 1993. On the identity of the cone types of the rat retina. Exp. Eye Res. 56, 375–377.
Ferrari, F.K., Samulski, T., Shenk, T., Samulski, R.J., 1996. Second-strand synthesis is a rate-limiting step for efficient transduction by recombinant adeno-associated virus vectors. J. Virol. 70, 3227–3234.
Fisher, K.J., Gao, G.P., Weitzman, M.D., DeMatteo, R., Burda, J.F., Wilson, J.M., 1996. Transduction with recombinant adeno-associated virus for gene therapy is limited by leading-strand synthesis. J. Virol. 70, 520–532.
Flannery, J.G., Greenberg, K.P., 2006. Looking within for vision. Neuron 50, 1–3.
Gal, A., Li, Y., Thompson, D.A., Weir, J., Orth, U., Jacobson, S.G., Apfelstedt-Sylla, E., Vollrath, D., 2000. Mutations in MERTK, the human orthologue of the RCS rat retinal dystrophy gene, cause retinitis pigmentosa. Nat. Genet. 26, 270–271.
Haruta, M., Sasai, Y., Kawasaki, H., Amemiya, K., Ooto, S., Kitada, M., Suemori, H., Nakatsuji, N., Ide, C., Honda, Y., Takahashi, M., 2004. In vitro and in vivo characterization of pigment epithelial cells differentiated from primate embryonic stem cells. Invest. Ophthalmol. Vis. Sci. 45, 1020–1025.
Iwamura, Y., Fujii, Y., Kamei, C., 2003. The effects of certain H(1)-antagonists on visual evoked potential in rats. Brain Res. Bull. 61, 393–398.
Jayandharan, G.R., Zhong, L., Li, B., Kachniarz, B., Srivastava, A., 2008. Strategies for improving the transduction efficiency of single-stranded adeno-associated virus vectors in vitro and in vivo. Gene Ther. 15, 1287–1293.
Jehle, T., Wingert, K., Dimitriu, C., Meschede, W., Lasseck, J., Bach, M., Lagreze, W.A., 2008. Quantification of ischemic damage in the rat retina: a comparative study using evoked potentials, electroretinography, and histology. Invest. Ophthalmol. Vis. Sci. 49, 1056–1064.
Kugler, S., Lingor, P., Scholl, U., Zolotukhin, S., Bahr, M., 2003. Differential transgene expression in brain cells in vivo and in vitro from AAV-2 vectors with small transcriptional control units. Virology 311, 89–95.
Lagali, P.S., Balya, D., Awatramani, G.B., Munch, T.A., Kim, D.S., Busskamp, V., Cepko, C.L., Roska, B., 2008. Light-activated channels targeted to ON bipolar cells restore visual function in retinal degeneration. Nat. Neurosci. 11, 667–675.
LaVail, M.M., Unoki, K., Yasumura, D., Matthes, M.T., Yancopoulos, G.D., Steinberg, R. H., 1992. Multiple growth factors, cytokines, and neurotrophins rescue photoreceptors from the damaging effects of constant light. Proc. Natl. Acad. Sci. U.S. A. 89, 11249–11253.
Li, G., Anderson, R.E., Tomita, H., Adler, R., Liu, X., Zack, D.J., Rajala, R.V., 2007. Nonredundant role of Akt2 for neuroprotection of rod photoreceptor cells from light-induced cell death. J. Neurosci. 27, 203–211.
Lin, B., Koizumi, A., Tanaka, N., Panda, S., Masland, R.H., 2008. Restoration of visual function in retinal degeneration mice by ectopic expression of melanopsin. Proc. Natl. Acad. Sci. U.S.A. 105, 16009–16014.
Lund, R.D., Adamson, P., Sauve, Y., Keegan, D.J., Girman, S.V., Wang, S., Winton, H., Kanuga, N., Kwan, A.S., Beauchene, L., Zerbib, A., Hetherington, L., Couraud, P.O., Coffey, P., Greenwood, J., 2001. Subretinal transplantation of genetically modified human cell lines attenuates loss of visual function in dystrophic rats. Proc. Natl. Acad. Sci. U.S.A. 98, 9942–9947.
Marc, R.E., Jones, B.W., Watt, C.B., Strettoi, E., 2003. Neural remodeling in retinal degeneration. Prog. Retin. Eye Res. 22, 607–655.
Marc, R.E., Jones, B.W., Anderson, J.R., Kinard, K., Marshak, D.W., Wilson, J.H., Wensel, T., Lucas, R.J., 2007. Neural reprogramming in retinal degeneration. Invest. Ophthalmol. Vis. Sci. 48, 3364–3371.
McCarty, D.M., Monahan, P.E., Samulski, R.J., 2001. Self-complementary recombinant adeno-associated virus (scAAV) vectors promote efficient transduction independently of DNA synthesis. Gene Ther. 8, 1248–1254.
Mullen, R.J., LaVail, M.M., 1976. Inherited retinal dystrophy: primary defect in pigment epithelium determined with experimental rat chimeras. Science 192, 799–801.
Nagel, G., Szellas, T., Huhn, W., Kateriya, S., Adeishvili, N., Berthold, P., Ollig, D., Hegemann, P., Bamberg, E., 2003. Channelrhodopsin-2, a directly light-gated cation-selective membrane channel. Proc. Natl. Acad. Sci. U.S.A. 100, 13940–13945.
Neitz, J., Jacobs, G.H., 1986. Reexamination of spectral mechanisms in the rat (*Rattus norvegicus*). J. Comp. Psychol. 100, 21–29.
Niwa, H., Yamamura, K., Miyazaki, J., 1991. Efficient selection for high-expression transfectants with a novel eukaryotic vector. Gene 108, 193–199.
Oesterhelt, D., Stoeckenius, W., 1973. Functions of a new photoreceptor membrane. Proc. Natl. Acad. Sci. U.S.A. 70, 2853–2857.
Oesterhelt, D., 1998. The structure and mechanism of the family of retinal proteins from halophilic archaea. Curr. Opin. Struct. Biol. 8, 489–500.
Papathanasiou, E.S., Peachey, N.S., Goto, Y., Neafsey, E.J., Castro, A.J., Kartje, G.L., 2006. Visual cortical plasticity following unilateral sensorimotor cortical lesions in the neonatal rat. Exp. Neurol. 199, 122–129.
Pittler, S.J., Baehr, W., 1991. Identification of a nonsense mutation in the rod photoreceptor cGMP phosphodiesterase beta-subunit gene of the rd mouse. Proc. Natl. Acad. Sci. U.S.A. 88, 8322–8326.
Sauve, Y., Girman, S.V., Wang, S., Lawrence, J.M., Lund, R.D., 2001. Progressive visual sensitivity loss in the Royal College of Surgeons rat: perimetric study in the superior colliculus. Neuroscience 103, 51–63.
Sauve, Y., Lu, B., Lund, R.D., 2004. The relationship between full field electroretinogram and perimetry-like visual thresholds in RCS rats during photoreceptor degeneration and rescue by cell transplants. Vis. Res. 44, 9–18.
Sineshchekov, O.A., Jung, K.H., Spudich, J.L., 2002. Two rhodopsins mediate phototaxis to low- and high-intensity light in *Chlamydomonas reinhardtii*. Proc. Natl. Acad. Sci. U.S.A. 99, 8689–8694.
Strettoi, E., Pignatelli, V., 2000. Modifications of retinal neurons in a mouse model of retinitis pigmentosa. Proc. Natl. Acad. Sci. U.S.A. 97, 11020–11025.
Strettoi, E., Porciatti, V., Falsini, B., Pignatelli, V., Rossi, C., 2002. Morphological and functional abnormalities in the inner retina of the rd/rd mouse. J. Neurosci. 22, 5492–5504.
Strettoi, E., Pignatelli, V., Rossi, C., Porciatti, V., Falsini, B., 2003. Remodeling of second-order neurons in the retina of rd/rd mutant mice. Vis. Res. 43, 867–877.
Sugano, E., Tomita, H., Ishiguro, S., Abe, T., Tamai, M., 2005. Establishment of effective methods for transducing genes into iris pigment epithelial cells by using adeno-associated virus type 2. Invest. Ophthalmol. Vis. Sci. 46, 3341–3348.
Suzuki, T., Yamasaki, K., Fujita, S., Oda, K., Iseki, M., Yoshida, K., Watanabe, M., Daiyasu, H., Toh, H., Asamizu, E., Tabata, S., Miura, K., Fukuzawa, H., Nakamura, S., Takahashi, T., 2003. Archaeal-type rhodopsins in *Chlamydomonas*: model structure and intracellular localization. Biochem. Biophys. Res. Commun. 301, 711–717.
Tomita, H., Ishiguro, S., Abe, T., Tamai, M., 1999. Administration of nerve growth factor, brain-derived neurotrophic factor and insulin-like growth factor-II protects phosphate-activated glutaminase in the ischemic and reperfused rat retinas. Tohoku J. Exp. Med. 187, 227–236.
Tomita, H., Sugano, E., Yawo, H., Ishizuka, T., Isago, H., Narikawa, S., Kugler, S., Tamai, M., 2007. Restoration of visual response in aged dystrophic RCS rats using AAV-mediated channelopsin-2 gene transfer. Invest. Ophthalmol. Vis. Sci. 48, 3821–3826.
Yokoyama, S., Radlwimmer, F.B., Kawamura, S., 1998. Regeneration of ultraviolet pigments of vertebrates. FEBS Lett. 423, 155–158.

Gene Therapy (2010), 1–9

www.nature.com/gt

ORIGINAL ARTICLE

Immune responses to adeno-associated virus type 2 encoding channelrhodopsin-2 in a genetically blind rat model for gene therapy

E Sugano[1], H Isago[1], Z Wang[1,2], N Murayama[1], M Tamai[3] and H Tomita[1,4,5]

We had previously reported that transduction of the channelrhodopsin-2 (ChR2) gene into retinal ganglion cells restores visual function in genetically blind, dystrophic Royal College of Surgeons (RCS) rats. In this study, we attempted to reveal the safety and influence of exogenous ChR2 gene expression. Adeno-associated virus (AAV) type 2 encoding ChR2 fused to Venus (rAAV-ChR2V) was administered by intra-vitreous injection to dystrophic RCS rats. However, rAAV-ChR2 gene expression was detected in non-target organs (intestine, lung and heart) in some cases. ChR2 function, monitored by recording visually evoked potentials, was stable across the observation period (64 weeks). No change in retinal histology and no inflammatory marker of leucocyte adhesion in the retinal vasculature were observed. Although antibodies to rAAV (0.01–12.21 $\mu g\,ml^{-1}$) and ChR2 (0–4.77 $\mu g\,ml^{-1}$) were detected, their levels were too low for rejection. T-lymphocyte analysis revealed recognition by T cells and a transient inflammation-like immune reaction only until 1 month after the rAAV-ChR2V injection. In conclusion, ChR2, which originates from *Chlamydomonas reinhardtii*, can be expressed without immunologically harmful reactions *in vivo*. These findings will help studies of ChR2 gene transfer to restore vision in progressed retinitis pigmentosa.
Gene Therapy advance online publication, 28 October 2010; doi:10.1038/gt.2010.140

Keywords: retinitis pigmentosa; channelrhodopsin-2; immunoreactivity; adeno-associated virus; retinal ganglion cells

INTRODUCTION

Retinitis pigmentosa (RP) is a group of diseases in which a gene mutation results in the death of photoreceptor cells. At present, approximately 40 genes have been identified as the causative agents (http://www.sph.uth.tmc.edu/retnet/; provided in the public domain by the University of Texas Houston Health Science Center, Houston, TX, USA). The initial visual impairment in patients with RP is night blindness, and patients lose their vision in the final stage of this disease following visual field loss.[1] Many trials have been conducted to identify agents that can protect photoreceptors and delay vision loss, but effective treatments have not been developed against progressed RP.

Although photoreceptor cells are often degenerated in the case of progressed RP, other inner neurons, including retinal ganglion cells (RGCs) are preserved.[2] It would be ideal to utilise the remaining retinal neurons to restore vision. We have been studying light-gated cation-selective membrane channel protein channelrhodopsin-2 (ChR2)[3] to induce photoreceptor function in retinal neurons such as RGCs[4,5] and ON bipolar cells.[6] We have already demonstrated that the responses induced by various stimulus frequencies (Hz) in ChR2-transduced rats are in no way inferior to those in normal rats,[7] as supported by the finding that ChR2-induced photocurrents are extremely fast.[8,9] Visual function was also well analysed by using transgenic rats with ChR2 transduction into RGCs: the spatial frequencies based on behavioural responses of photoreceptor-degenerated ChR2 transgenic rats were the same as those of normal rats.[10] These studies indicate that transfer of the ChR2 gene into the remaining retinal neurons is a useful method for restoring vision in progressed RP.

However, for clinical application of ChR2 therapy, some problems must be considered. First, this approach is a gene therapy. An immune response (mostly a problem with adenovirus- and herpes simplex virus-derived vectors)[11] may be caused by adeno-associated virus (AAV) and its incorporation into the host genome may lead to de-repression of tumour suppression genes.[12–14] Second, ChR2 is a protein originating from *Chlamydomonas reinhardtii*. It is important to study the systemic responses on virus vector application and long-term expression of the transgene product in humans. In this study, to reveal the safety and influence of exogenous ChR2 gene expression, we investigated the functional stability of the ChR2 gene and the possibility of harmful immune reactions caused by this gene therapy in a Royal College of Surgeons (RCS) rat model of RP.

RESULTS

Recording of visually evoked potentials (VEPs) in RCS rats

Although RGCs are maintained in aged RCS (*rdy/rdy*) rats, VEPs would be abolished because of the loss of light-evoked synchronous activities by photoreceptor cells. Indeed, VEPs were not evoked even

[1]Department of International Advanced Interdisciplinary Research, Institute for International Advanced Research and Education, Tohoku University, Sendai, Japan; [2]Japan Foundation for Aging and Health, Aichi, Japan; [3]School of Medicine, Tohoku University, Sendai, Japan; [4]United Centers for Advanced Research and Translational Medicine, School of Medicine, Tohoku University, Sendai, Japan and [5]Innovation of New Biomedical Engineering Center, Tohoku University, Sendai, Japan
Correspondence: Dr H Tomita, Department of International Advanced Interdisciplinary Research, Institute for International Advanced Research and Education, Tohoku University, 4-1 Seiryo-machi, Aoba-ku, Sendai 980-8575, Japan.
E-mail: hiroshi-tomita@iiare.tohoku.ac.jp
Received 9 June 2010; revised 29 August 2010; accepted 7 September 2010

by the maximum flash of the light-emitting diode in any of the 6-month-old RCS (*ryd/rdy*) rats. After confirmation of the loss of photoreceptor-derived function, AAV encoding ChR2 fused to Venus (rAAV-ChR2V) was administered by intra-vitreous injection into the left eye. The right eye was not treated and served as the control. At 2 weeks after the injection, VEPs were recorded in the right visual cortex. The amplitude peaked at 8 weeks but remained stable until 64 weeks after the injection (Figure 1). There was no recording from the left side of the visual cortex (data not shown). We could not record for longer periods than 64 weeks because the lifespan of RCS rats is about 2 years.

Viral dissemination to the organs

To determine systemic dissemination of rAAV after the injection, total ribonucleic acids were isolated from each organ after 6 months of rAAV-ChR2V administration. No rAAV-derived Venus expression was detected by reverse transcription-polymerase chain reaction (RT-PCR) analysis from the brain, liver, spleen and kidney (Figure 2). As expected, we detected the appropriate Venus protein expression from the rAAV-transduced retinas. Venus expression was unexpectedly detected in other organs (heart, lung and intestine) in some cases.

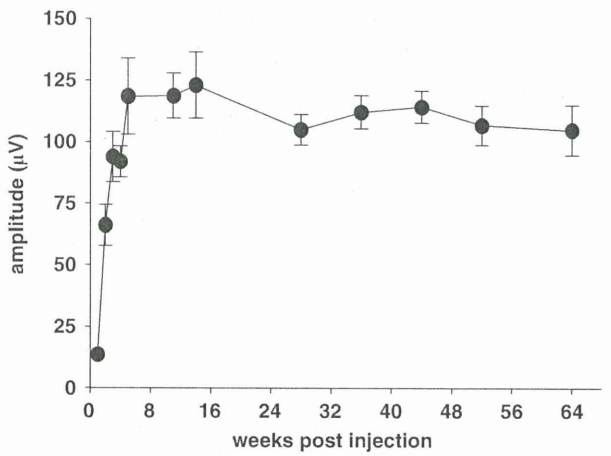

Figure 1 Long-term functional analysis of photosensitivity following ChR2 gene transfer by intra-vitreous injection of rAAV-ChR2V in 6-month-old RCS (*rdy/rdy*) rats. A blue LED (wavelength, 435–500 nm; peak, 470 nm) was flashed for 20 ms at 2.6 mW cm^{-2} and time-dependent improvements in the amplitude of the VEPs were recorded. After peaking at 8 weeks of administration, the amplitude remained stable for 64 weeks post-injection.

Histological examination of rAAV-ChR2V-treated retina

The rAAV-derived gene expression was investigated by observing whole-mounted retina. At 6 months after rAAV administration, the expression of ChR2V or Venus was observed by fluorescence microscopy (Figure 3). ChR2V was expressed in the plasma membrane of the retinal cells; on the other hand, Venus expression was observed in the cytoplasm of the rAAV-Venus-injected retina. Both of the rAAV-derived proteins were expressed all over the retina, and there was some deflection of the retinal expression.

To assess the side effects of ChR2 gene transfer by using rAAV, histological studies were performed on paraffin-embedded and frozen sections. There was no obvious difference in the retinal morphology between the ChR2-injected and the age-matched untreated RCS (*rdy/rdy*) rats (Figures 4a and b). However, intra-vitreous injection of lipopolysaccharide, which resulted in endotoxin-induced uveitis (EIU), in the RCS (+/+) rats caused substantial migration of inflammatory cells, mainly polymorphonuclear leucocytes, in the neural retina and vitreous humour (Figure 4d).

When the retinal activities were studied in frozen sections by immunohistochemistry (Figure 5), glial fibrillary acidic protein (GFAP) expression was restricted to the ganglion cell layers in the rAAV-ChR2V-treated retina (Figure 5c); however, GFAP expression was observed throughout the inner half of the retina in the untreated RCS (Figure 5b) and rAAV-Venus-injected RCS (Figure 5d) rats. Nuclear factor-κB (NF-κB) expression was restricted to the ganglion cell layers in all the tested RCS rats, but it was markedly high in the rAAV-ChR2V-treated retinas (Figure 5h).

Effects of rAAV-ChR2V treatment on leucocyte adhesion in the retinal vasculature

The retinal adherent leucocytes were imaged by perfusion labelling with fluorescein isothiocyanate-coupled concanavalin A. According to a report of Koizumi *et al.*,[15] leucocyte adhesion is significantly elevated

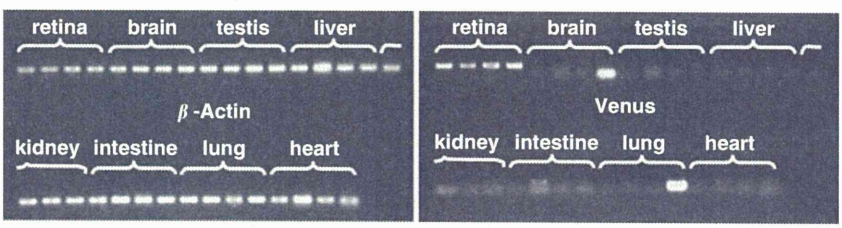

The expression of venus protein, which was carried by rAAV

	retina	brain	testis	liver	kidney	intestine	lung	heart
Sample1	+++	-	-	-	-	-	-	-
Sample2	+++	-	-	-	-	++	-	+
Sample3	+++	-	-	-	-	-	-	+
Sample4	+++	-	-	-	-	-	+	+

Abbreviations : -, No expression; +, Light expression; + + , Moderate expression; + + + , Intense expression;

Figure 2 Virus dissemination to the organs. At 6 months after the administration of rAAV-ChR2V, total ribonucleic acid was extracted from the retina, brain, testis, liver, kidney, intestine, lung and heart. The rAAV-derived gene was investigated by using RT-PCR analysis. As expected, a high copy number of the rAAV-derived gene expression was detected in the retina. The gene expression was also detected in the heart, lung and intestine in some cases.

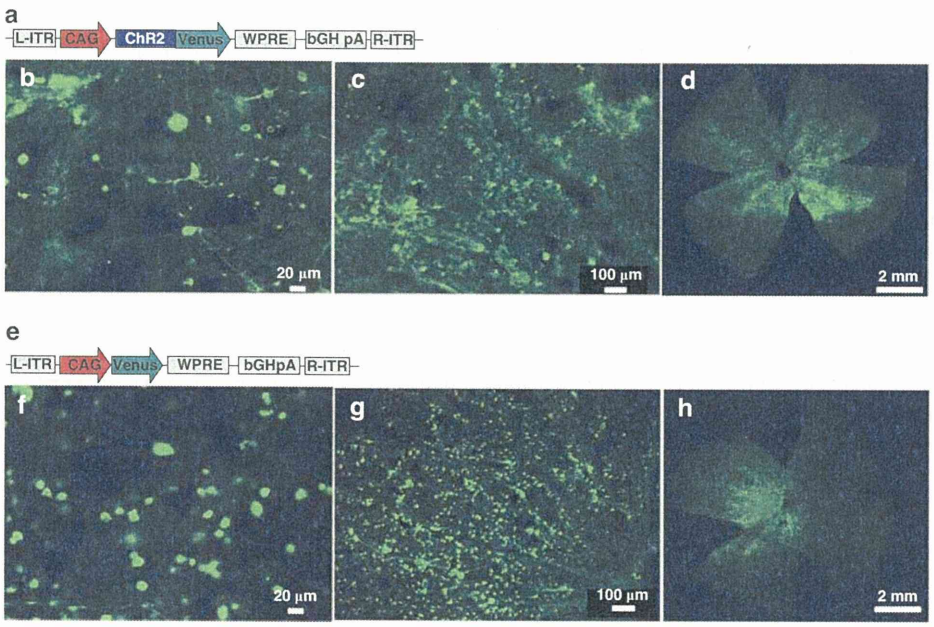

Figure 3 Expression profiles of the rAAV-derived proteins in the retina. Construction of the rAAV vector expressing ChR2V (**a**) and Venus (**e**) is illustrated. After 6 months of intra-vitreous injection, the rAAV-derived protein expression in whole-mounted retinal samples was observed by fluorescence microscopy. ChR2V expression was observed in the membrane (**b–d**) and Venus was expressed in the cytoplasm (**f–h**) of the retinal cells.

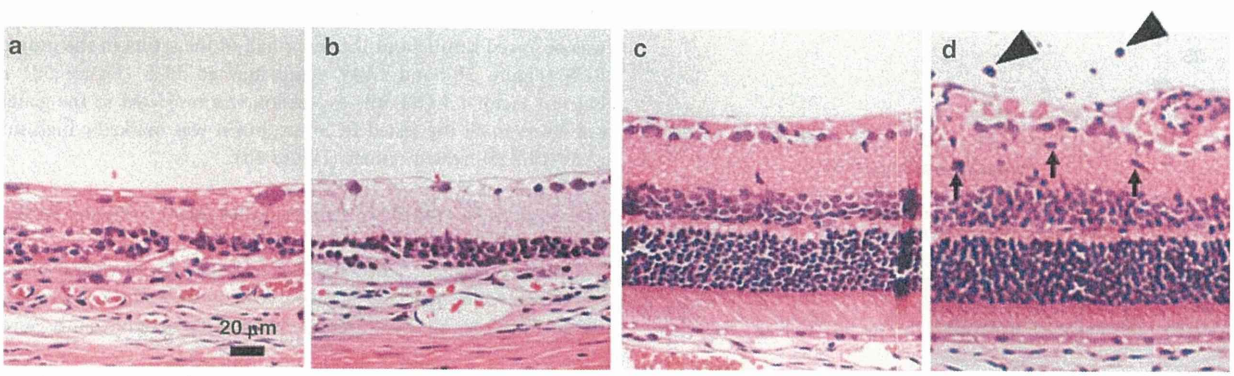

Figure 4 Histological examination of rAAV-ChR2V-treated retina. rAAV-ChR2V was administered by intra-vitreous injection into the left eye of RCS (*rdy/rdy*) rats. After 64 weeks, their right (control) (**a**) and left (**b**) eyeballs were enucleated and stained with hematoxylin and eosin. As a model of inflammation, age-matched RCS (+/+) rats were administered lipopolysaccharide (LPS) by intra-vitreous injection and their eyeballs were enucleated after 48 h. Retinal sections of untreated RCS (+/+) (**c**) and the LPS-treated (**d**) rats were studied. Substantial infiltration of inflammatory cells, which were mainly PMNLs in the neural retina (arrow) and vitreous humour (arrowhead), was observed in the retina of the LPS-treated rats.

after the development of EIU. Our study demonstrated that EIU caused leucocyte adhesion in the retinal venules (Figures 6c and d). However, there was no difference in leucocyte adhesion between the untreated (Figure 6a) and the rAAV-ChR2V-injected (Figure 6b) RCS rats, which had received the rAAV injection 1 year previously.

Humoral immune responses to the viral vector and transgene

To assess the possibility of a systemic humoral immune response to the viral vector or transgene, we determined the antibody levels against the rAAV2 capsid and ChR2 in serum by enzyme-linked immunosorbent assay. In the rAAV-ChR2V-injected rats, rAAV2 capsid-specific antibodies were detected and showed the maximum production at 2 months after injection (0.01–12.21 $\mu g\,ml^{-1}$; Figure 7a). However, the titre was extremely low in this study compared with that in a previous report of intramuscular injection of AAV2 (200–400 $\mu g\,ml^{-1}$).[16] The titre against the ChR2 protein was the maximum at 6 months post-injection. However, this level was also low (0–4.77 ± 2.55 $\mu g\,ml^{-1}$) compared with the antibody level in serum of the immunized rabbit (1442.34 $\mu g\,ml^{-1}$), which received a peptide injection to produce antibody to ChR2 forcibly (Figure 7b).

Analysis of T-lymphocyte subsets

Total T lymphocytes were gated with positive staining of anti-CD3. Then, the population of lymphocytes was confirmed by forward scatter (cell size) versus side scatter (cell granularity). Analysis of T lymphocyte subsets, namely $CD4^+$ (T helper cells), $CD8^+$ (cytotoxic

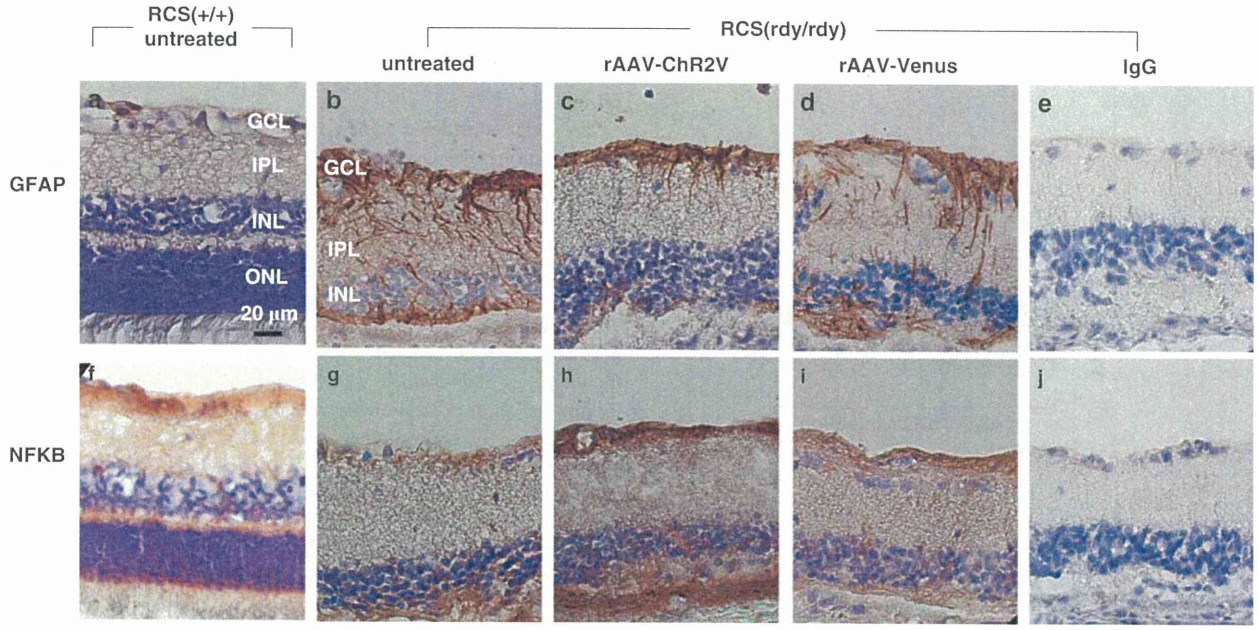

Figure 5 Changes in the protein immunoreactivities in the retina. Untreated RCS (+/+) (**a** and **f**) and RCS (*rdy/rdy*) (**b** and **g**) rats were used as the controls. rAAV-Venus (**d** and **i**) or rAAV-ChR2V (**c** and **h**) was administered by intra-vitreous injection into the left eye of RCS (*rdy/rdy*) rats. After 64 weeks, their eyeballs were enucleated. All the RCS rats were of the same age at the time of enucleation (2.2 years). As the negative control for staining, the first antibodies were replaced with non-immune mouse immunoglobulin G (**e** and **j**). DNA was counterstained with 4', 6-diamidino-2-phenylindole. GFAP expression was restricted to the ganglion cell and nerve fibre layers of the ChR2V-treated retina (**c**); however, it was observed throughout the inner half of the retina in the untreated RCS (**b**) and rAAV-Venus-injected RCS (**d**) rats. Nuclear factor-κB expression was restricted to the ganglion cell layers in all the tested RCS rats, but it was markedly high in the ChR2V-treated retina (**h**).

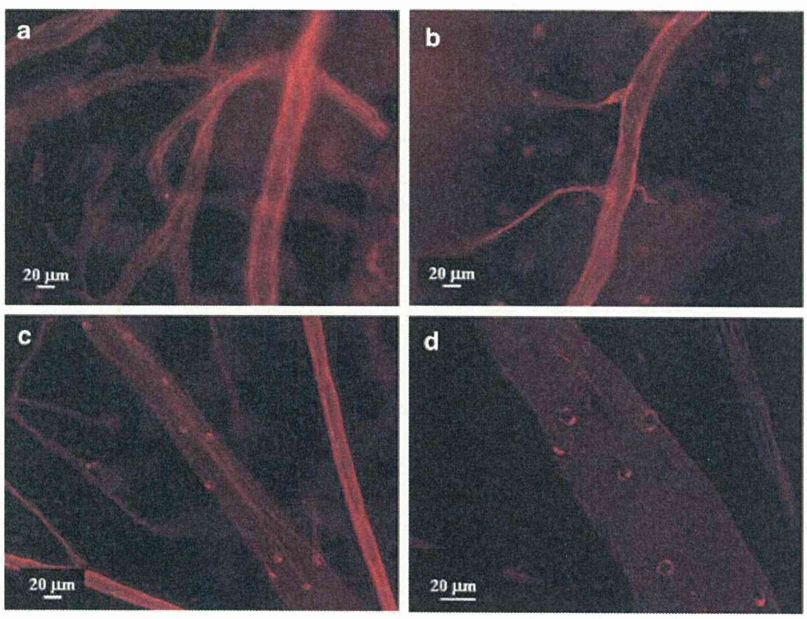

Figure 6 Adverse effect of rAAV-ChR2V treatment on retinal leucocyte adhesion. To study the adverse effect of ChR2 treatment in RCS rats, their retinas were examined after 1 year of rAAV-ChR2V injection. As a model of inflammation, RCS (+/+) rats received an intra-vitreous injection of lipopolysaccharide (LPS) and were examined 48 h after the injection. Flat-mounted retinas labelled with concanavalinA lectin showed increased number of adherent leucocytes in the retinal vessels of the LPS-injected rats (**c**) compared with the untreated (**a**) and rAAV-ChR2V-injected (**b**) rats. High-magnification photography of the LPS-treated retinal vessels showed leucocyte adhesion more clearly (**d**).

cells) and $CD4^+CD25^+$ (T regulatory cells), was performed. The $CD4^+/CD8^+$ ratio is a known indicator of the immunoregulatory status.[17,18] Our results demonstrated that the $CD4^+/CD8^+$ ratio after 1 week of the rAAV injection was higher than the pre-injection ratio (Figure 8a). This increase occurred in the case of both the rAAV-Venus and rAAV-ChR2V injections. In addition, the $CD4^+/CD8^+$ ratio only 1

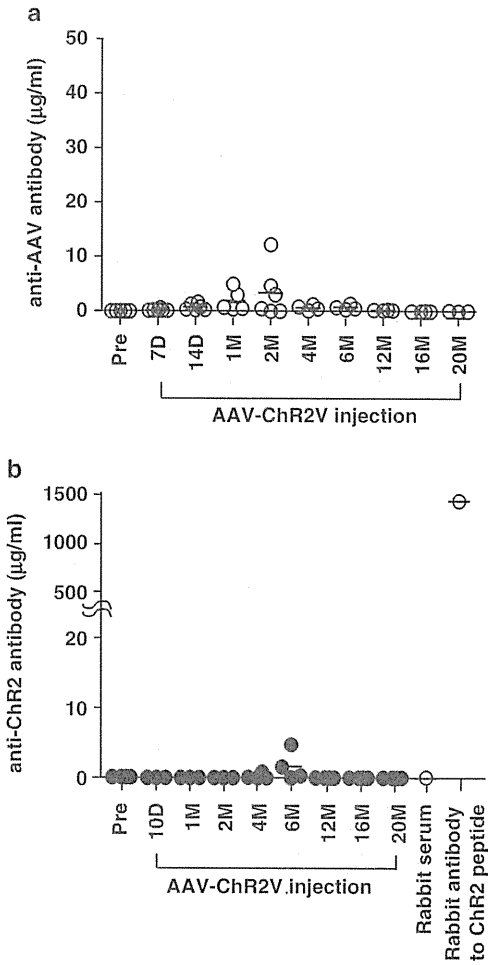

Figure 7 Humoral immune responses to the viral vector and transgene. Production levels of the antibodies to the AAV2 vector (**a**) and the therapeutic gene, ChR2 (**b**), were studied in RCS rats following a single intra-vitreous injection of rAAV-ChR2V. The time after injection is indicated. The antibody levels against both AAV2 and ChR2 were quite low compared with the antibody levels in serum of an immunized rabbit, which were considered as the effective dose to react with antigens.

month after the rAAV-ChR2V injection was higher than that before the injection. These data suggested that a change in the inflammation status occurred from 1 week to 1 month after rAAV administration. After this period, the ratios decreased to the pre-injection value and were stable for 1 year. To assess the inflammation status, we studied T regulatory cells. As shown in Figure 8b, a significant increase in the number of $CD4^+CD25^+$ cells was observed at 1 week after the rAAV-Venus and rAAV-ChR2V injections compared with the numbers before the injections. There was no significant difference in the inflammation status between the rAAV injections. As a positive control of inflammation, EIU also increased the population of $CD4^+CD25^+$ cells, which is consistent with a report by Toda *et al.*[19]

DISCUSSION

The results of this study demonstrate that the strategy of restoration of vision and light responses in photoreceptor-degenerated RCS (*rdy/rdy*) rats by rAAV-ChR2V administration was technically feasible and safe. Most importantly, ChR2 function, which was confirmed by measuring VEPs, was not reduced over the whole observation period after rAAV-ChR2V administration (Figure 1). A single administration of rAAV-ChR2V restored the light sensitivity over the lifespan of the rat model.

The eye is considered to be an immunologically protected space.[20] This immune privilege is the result of multiple layers and mechanisms, including the blood–retina barrier and other physical barriers, such as the immunosuppressive microenvironment against deviant systemic immunity, that limit the production of pro-inflammatory effector cells. We predicted that systemic dissemination of a virus would be limited by these immune systems after intra-vitreous injection. To investigate the systemic dissemination of rAAV, ribonucleic acids were isolated from each organ and the expressions of the Venus protein, which was fused to rAAV-ChR2, were studied (Figure 2). Venus expression was notable in the retina. Contrary to our expectations, the expression was also detected in the intestine, lung and heart in some cases. The RCS (*rdy/rdy*) animal model, which genetically causes loss of photoreceptors, is reported to have some breakdown of the blood–retina barrier or other mechanisms.[21–24] Therefore, the rAAV vector might have been disseminated to the other organs. Supporting this hypothesis, the efficiency of rAAV-derived gene transfer was higher in RCS rats than in normal rats (data not shown). This result suggests that some breakdown of the retinal barriers increased the permeability to rAAV.

The genomes transferred by rAAV tend to persist in cells mainly in an episomal, non-integrated form.[25] The transferred genomes in episomal form are diluted by cell division. However, when rAAV-carried genomes are inserted into chromosomes of cells with high proliferation ability, the genomes are preserved. There were some differences in gene delivery by rAAV among the samples obtained from the intestine, lung and heart. These differences might be the result of differences in the insertion forms of the rAAV genomes.

In gene therapy, tumour formation caused by the insertion of a transgene into the genome has been reported.[12–14] We did not observe tumour formation in any of the rats that received the rAAV injections (data not shown). For more information regarding tumour formation, further studies are needed by using methods such as Northern blotting, integration site analysis[26] and oncogene analysis.

We also investigated the inflammatory responses caused by the gene transfer by using the EIU model as a positive control of inflammation. EIU caused ocular inflammation, including leucocyte infiltration into the vitreous humour (Figure 4d) and leucocyte adhesion to the retinal vessels (Figures 6c and d). These findings are consistent with those of previous reports.[15,27] However, we did not observe such inflammatory cells in the retinas treated with rAAV-Venus or rAAV-ChR2V. Therefore, rAAV-ChR2V administration did not induce inflammation arising from bacterial infection.

GFAP is reportedly expressed because of gliosis and hypertrophy of macroglial cells.[28] Moreover, GFAP is expressed in astrocytes in the retina usually, but in Müller cells under pathological or stress conditions.[29] GFAP was also reported to be upregulated in the brain astrocytes during the inflammatory response.[30] Beurel and Jope[31] revealed that GFAP upregulation is caused by the production of the inflammatory cytokine interleukin-6. The absence of GFAP upregulation by viral injection (Figures 5b–d) demonstrates the lack of glial activation derived from inflammation. Our study showed that GFAP was expressed throughout the retina in the untreated RCS rats and that the expression was decreased and restricted by the rAAV-ChR2V injection (Figure 5c). These results reveal that activation of RGCs by ChR2 may have a protective effect on the inner retina.[32,33] NF-κB expression in the retina was restricted to the ganglion cell layers in all

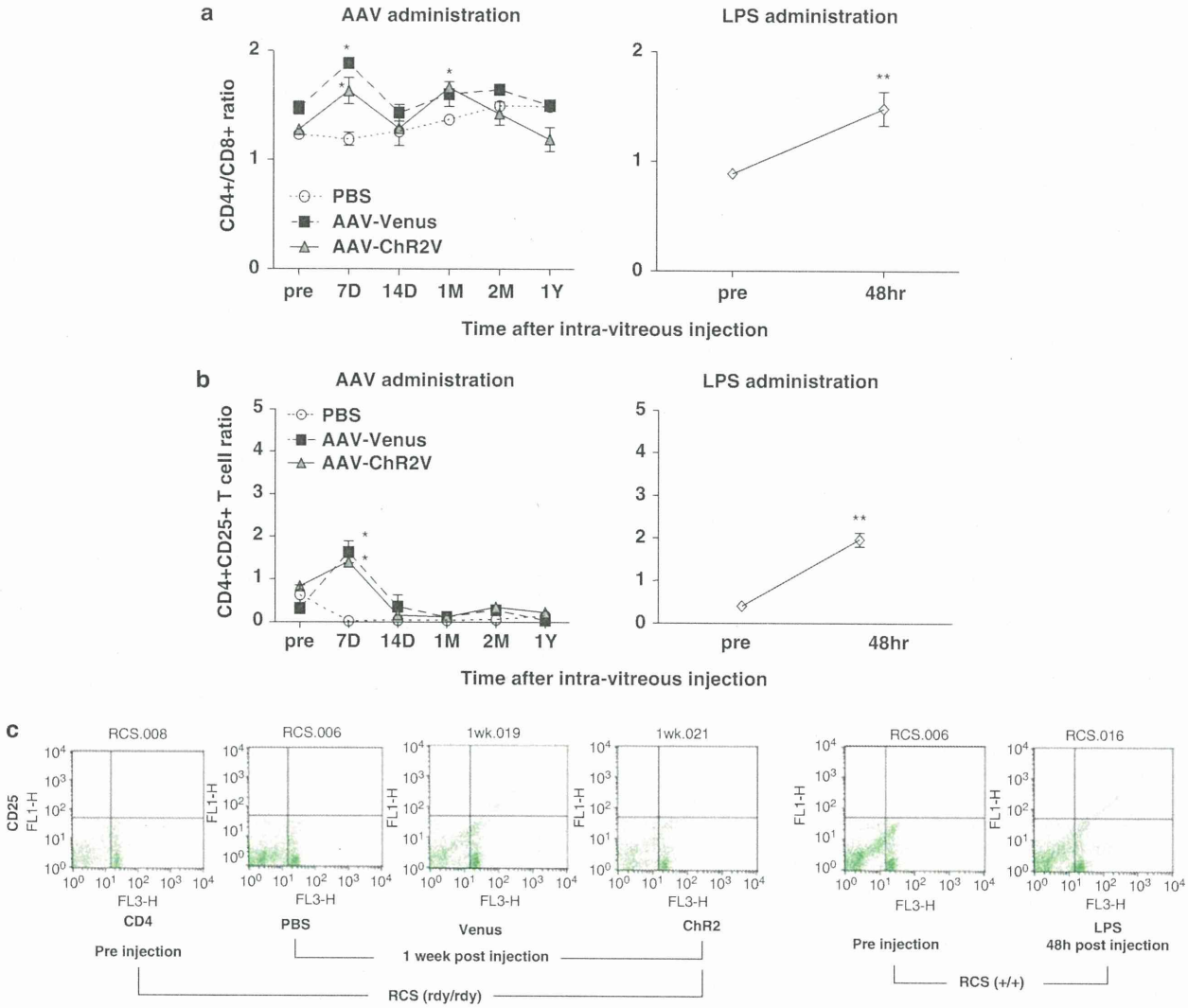

Figure 8 T-cell ratio in the peripheral blood. Lymphocytes were isolated from the peripheral blood before and after injection of PBS, rAAV-Venus or rAAV-ChR2V. The lymphocytes were incubated with anti-T-cell receptor-associated CD3, anti-CD4 and anti-CD8a mAbs, and analysed by flow cytometry. The blood of lipopolysaccharide-administrated rats as a positive control of inflammation was also analysed. The T-cell ratio of $CD4^+/CD8^+$ (**a**) and $CD4^+CD25^+$ (T regulatory cells) (**b**) was calculated. (**c**) Representative data of T regulatory analysis are indicated. All data are represented as the mean (s.d.) of four to seven animals.

the experiments and there was no staining of the other inner retinal cells, which was caused by stress.[34] We also demonstrated the potent expression of NF-κB p65 in the rAAV-ChR2V-injected retinas. These results are consistent with reports that constitutive NF-κB activity is the result of ongoing synaptic activity.[35,36]

The T-lymphocyte analysis demonstrated that the $CD4^+/CD8^+$ ratio was higher in all the rAAV-treated rats at 1 week after the injection than before the injection, and in the rAAV-ChR2V-treated rats, the ratio was high at 1 month after injection (Figure 8a). However, these increases were transient and returned to the pre-injection level. This expansion allows cross-talk between different types of cells in the ongoing immune response.[17] Kim and Lim[18] reported that $CD4^+/CD8^+$ expansion is caused by bacterial infection. After 1 week, the ratio increased in all the rAAV-injected rats. Thus, there might have been some immune reactions such as antigen presentation to rAAV. At 1 month after the rAAV-ChR2V injection, the ratio increased again. As shown in Figure 1, the maximum ChR2 function was recorded at 1 month in the visual cortex first. Thus, some immune reactions might have been induced by increased ChR2 expression but were well tolerated at 2 months after the injection.

Currently, the best characterized regulatory cells are $CD4^+CD25^+$ T cells.[37] These cells can suppress host immune responses and modulate the immune responses in autoimmune diseases, allergy, transplantation and infectious diseases.[38,39] CD25, an interleukin-2 receptor, is reported to be an inflammation marker on $CD4^+$ lymphocytes.[18] In the EIU experiment, we observed expansion of $CD4^+CD25^+$ cells, which is consistent with the report by Toda *et al.*[19] A significant increase in the number of $CD4^+CD25^+$ cells was observed in both the rAAV-Venus and the rAAV-ChR2V rats at 1 week after the injections compared with the pre-injection values (Figure 8b), although there was no significant difference in the results between the rAAV-Venus and the rAAV-ChR2V injections.

These results demonstrate that the inflammation-like immunological reaction was caused by AAV and not by ChR2.

To assess the possibility of a systemic humoral immune response to the viral vector or transgene product, we measured the antibody levels of the rAAV2 capsid and ChR2 in serum by enzyme-linked immunosorbent assay. Intra-vitreous injection caused relatively little antibody production (Figure 7a) compared with the different route of AAV injection used by Zhang *et al.*[16] Li *et al.*[40] demonstrated that a single intra-vitreous injection of AAV2 causes increased AAV antibody production at 2 months after injection. Our data are consistent with their report in terms of the timing of increase and the amount of antibody production (Figure 7a). We anticipated that ChR2 expression would cause antibody production because ChR2 is not inherent to humans. However, the production levels were relatively low (Figure 7b) and were insufficient to induce a humoral immune response.

In conclusion, an immune reaction can be caused by AAV administration and ChR2 protein expression, but will be well tolerated. It should be noted that the experiments were performed in rats and cannot be directly extrapolated to humans, who constitute a far more immunologically heterogeneous population. However, these findings will help studies of ChR2 gene transfer to restore vision in progressed RP.

MATERIALS AND METHODS

Animals

In total, 59 (6-month-old male) RCS rats (43 dystrophic (*rdy/rdy*)); 16 non-dystrophic (+/+) were used in this study (Table 1). The animals were maintained and used in accordance with the ARVO Statement for the *Use of Animals in Ophthalmic and Vision Research and the Guidelines for Animal Experiments of Tohoku University.* All the animal experiments were conducted with the approval of the Animal Research Committee, School of Medicine, Tohoku University. To compare the functions, the control and treated rats were age-matched in each experiment.

Induction of EIU

As a model of ocular inflammation,[41] RCS (+/+) rats received a single intra-vitreous injection of 5 μg lipopolysaccharide from *Escherichia coli* (055:B5; Sigma, St Louis, MO, USA) in 5 μl phosphate-buffered saline (PBS) to cause EIU. After 48 h of lipopolysaccharide administration, the inflammation status was studied.

Preparation of AAV vector carrying the ChR2 gene construct

The *N*-terminal fragment (residues 1–315) of ChR2 (GenBank accession no. AF461397) was fused to a fluorescent protein, Venus, in frame at the end of the ChR2-coding fragment described previously.[5] The ChR2V or Venus gene was introduced into the *Eco*RI and *Hin*dIII sites of the 6P1 plasmid.[42] The synapsin promoter was exchanged for a hybrid cytomegalovirus enhancer/chicken β-actin promoter,[42] and AAV-ChR2V and AAV-Venus were constructed. The pAAV-RC and p-Helper plasmids were obtained from Stratagene (La Jolla, CA, USA). Semi-confluent 293T cells on 15-cm plates were co-transfected with split-packaging plasmids—AAV-ChR2V (or AAV-Venus), pAAV-RC and p-Helper—by using a calcium phosphate-based protocol according to the manufacturer's instructions (Agilent Technologies, La Jolla, CA, USA). The rAAV vectors (rAAV-ChR2V, rAAV-Venus) were purified by using the method of Auricchio *et al.*[43–45]

rAAV vector injection

The rAAV-ChR2V or rAAV-Venus vector was administered by intra-vitreous injection into the left eye of 6-month-old RCS (*rdy/rdy*) rats. In brief, the rats were anaesthetised by intramuscular injection of a mixture of ketamine (66 mg ml^{-1}) and xylazine (33 mg kg^{-1}). Under an operating microscope, the conjunctiva was incised to expose the sclera. A total volume of 5 μl of vector suspension at a concentration of 5×10^{12} genomic particles per μl was administered by intra-vitreous injection through the ora serrata with a 10-μl Hamilton syringe and a 32-gauge needle (Hamilton Company, Reno, NV, USA).

Recording of VEPs

VEPs were recorded by using Neuropack MEB-9102 (Nihon Kohden, Tokyo, Japan). The method of recording was derived from a combination of protocols used by Papathanasiou *et al.*[46] and Iwamura *et al.*[47] In brief, at least 7 days before the experiments, recording electrodes (silver–silver chloride) were placed epidurally on each side 7 mm behind the bregma and 3 mm lateral to the midline, and a reference electrode was placed epidurally on the midline 12 mm behind the bregma. Under ketamine–xylazine anaesthesia, the pupils were dilated with 1% atropine and 2.5% phenylephrine hydrochloride. The ground electrode clip was placed on the tail. Photic stimuli of 20-ms duration were applied at a frequency of 0.5 Hz and generated by pulse activation of a blue light-emitting diode with light-emitting wavelengths in the range 435–500 nm (peak, 470 nm). A total of 100 consecutive response waveforms were averaged for the VEP measurements.

Table 1 The Number of samples examined in this study

	VEP	*PCR*	*Expression in retina (whole mount)*	*Histology (HE)*	*Immuno-histochemistry*	*Leukocyte adhesion*	*Antibody detection*	*Flow cytometry*	*Total (n)*
No treatment (+/+)				3	3	3			9
Pre-treatment (+/+)								7	7
LPS administration (+/+)				3		4		7	
No treatment (*rdy/rdy*)				3	3	3			9
Pre-injection for PBS (*rdy/rdy*)								4	4
After PBS injection (*rdy/rdy*)								4	
Pre-injection for rAAV-Venus (*rdy/rdy*)								4	10
After rAAV-Venus injection (*rdy/rdy*)			3		3			4	
Pre-injection for rAAV-ChR2V (*rdy/rdy*)	20						3–6	4	20
After rAAV-ChR2V injection (*rdy/rdy*)	20	4	3	3	3	3	3–6	4	

Abbreviations: ChR2V, channelrhodopsin-2 fused to Venus; HE, hematoxylin and eosin; LPS, lipopolysaccharide; PBS, phosphate-buffered saline; PCR, polymerase chain reaction; rAAV, adeno-associated virus type 2; VEP, visually evoked potential.

Ribonucleic acid isolation and rAAV-derived protein detection by RT-PCR analysis

Total ribonucleic acids were extracted (TRIreagent; Sigma) from the retina, brain, lung, testis, liver, kidney, intestine, lung and heart. cDNA was synthesised (First-Strand cDNA synthesis kit; GE Healthcare, Piscataway, NJ, USA) and the tracer fusion protein, Venus, expression was investigated by using a semi-quantitative RT-PCR method. As the individual internal control, we performed PCR with β-actin. The primer sequences were as follows: 5′-TCATGAAGTGT GACGTTGACATCCGT-3′ (sense) and 5′-CCTAGAAGCATTTGCGGTGCAC GATG-3′ (antisense) for β-actin; 5′-GACGTAAACGGCCACAAGTT-3′ (sense) and 5′-GAACTCCAGCAGGACCATGT-3′ (antisense) for Venus. Following electrophoresis on 1.0% agarose gel, DNA was detected by staining with GelRed (Biotium, Inc., Hayward, CA, USA).

Histology

After death, the eyeballs were enucleated, immersed in 4% paraformaldehyde in PBS overnight at 4 °C and embedded in paraffin. Serial sections (4 μm) of whole eyes were cut sagittally, through the cornea and parallel to the optic nerve, and stained with haematoxylin and eosin. Microscopic examination of the sections was then performed (AxioImager A1; Carl Zeiss, Tokyo, Japan).

The ChR2V expression profile in the retina was studied according to the method we previously described.[5] In brief, the eyes were fixed and the retinas were flat-mounted on slides. Venus fluorescence was visualised under a fluorescence microscope (BZ-9000; Keyence Corp., Osaka, Japan).

Immunohistochemistry

Rat eyes were fixed overnight at 4 °C in 4% paraformaldehyde in PBS (pH 7.4). The retinas were rinsed with PBS and immersed in 10, 20 and 30% sucrose in PBS at 4 °C. Samples were embedded in optimal cutting temperature compound (Sakura, Tokyo, Japan) under liquid nitrogen and stored at −80 °C. Cryosections (10 μm) of tissue were mounted on slides and air dried. Then, retinal sections were washed with PBS and treated for 15 min with 0.3% H_2O_2 in methanol. After washing with PBS, the sections were incubated with mouse anti-rat NF-κB p65 (C-20) antibody (1:200; Santa Cruz Biotechnology, Santa Cruz, CA, USA) and mouse anti-rat GFAP antibody (1:250; Nihon Millipore, Tokyo, Japan) in antibody diluent buffer (0.05% Tween-20, 3% bovine serum albumin and 3% goat serum in PBS) overnight at 4 °C. After washing with 0.05% Tween-20 in PBS, the sections were incubated with horseradish peroxidase-conjugated goat anti-mus immunoglobulin G as the secondary antibody for 1 h at room temperature. After washing with TBST (150 mM NaCl, 0.1% Tween-20 in 20 mM Tris-HCl), the immunohistochemical reactions were visualised by using an Envision DAB kit (Dako, Tokyo, Japan). The sections were counterstained with haematoxylin. As a negative control for staining, the first antibodies were replaced with non-immune mouse immunoglobulin G (Dako). The sections were observed under a microscope (AxioImager A1; Carl Zeiss).

Lectin labelling of the retinal vasculature and adherent leucocytes

Leucocytes adhering to the retinal vasculature were imaged by perfusion labelling with fluorescein isothiocyanate-coupled concanavalin A lectin (Vector Laboratories, Burlingame, CA, USA).[27] After deep anaesthesia, the chest cavity was opened, a 20-gauge perfusion cannula was introduced into the aorta and a part of the liver was excised. After injection of 20 ml PBS to remove erythrocytes and non-adherent leucocytes, 20 ml of fluorescein isothiocyanate-conjugated concanavalin A lectin (40 μg ml^{-1}) was injected. Residual unbound concanavalin A was removed with PBS perfusion. After the eyeballs were enucleated, the retina was flat-mounted and imaged under a fluorescence microscope (Axiovert 40; Carl Zeiss).

Enzyme-linked immunosorbent assay

To detect serum antibodies to the rAAV2 capsid and the transgenic protein, ChR2, we coated enhanced protein-binding enzyme-linked immunosorbent assay plates with 10^9 viral particles per well of rAAV2 in 100 μl of 0.1 M sodium carbonate buffer (pH 9.6) and with 0.2 μg per well peptide coding for ChR2 by using a peptide coating kit (TaKaRa, Shiga, Japan) at 4 °C overnight. The wells were blocked with 10% fetal bovine serum-0.1% Tween in PBS for 30 min at 37 °C. Then, serum dilutions were added and incubated for 4 °C overnight. Dilutions of a rabbit anti-AAV2 capsid protein (American Research Product, Belmont, MA, USA) and a rabbit anti-ChR2 protein (TaKaRa) served as positive controls. The plates were incubated with horseradish peroxidase-conjugated anti-rabbit immunoglobulin G or anti-rat immunoglobulin G at 37 °C for 1 h in the presence of 3% goat serum. The reactions were visualised by adding one-step tetramethylbenzidine substrate (Promega, Tokyo, Japan). The reactions were stopped by adding 1 N HCl and read at 450 nm with a VERS Amax plate reader (Molecular Devices, Osaka, Japan). Each value was determined in triplicate.

Analysis of T lymphocytes

Peripheral blood $CD4^+$ cells have a central role in regulating the cell-mediated immune response to infection. Often known as helper T cells, they act on other cells of the immune system to promote various aspects of the immune response, including immunoglobulin isotype switching and affinity maturation and enhanced activity of natural killer cells and cytotoxic T cells. $CD4^+$ cells also act by releasing cytokines in response to antigenic stimulation. One of the major roles of $CD4^+$ cells is the activation of macrophages. During the course of hepatitis C virus infection, two different immunological statuses can be observed. In the acute phase of infection, $CD4^+$ helper T cells contribute to the induction and maintenance of a functional $CD8^+$ cell response. In the chronic phase, T regulatory ($CD4^+CD25^+$) cells suppress $CD8^+$ cell responses, and thereby help the virus to persist.[48] It is important to calculate these ratios to observe the immunological status.

Before and after the rAAV injection, peripheral blood was collected from the tail vein. Lymphocytes were isolated with PharmLyse (BD Bioscience, San Jose, CA, USA). After isolation, a mixture of monoclonal antibodies (mAbs) specific for CD3 (conjugated with Alexa Fluor 647; AbD Serotec, Oxford, UK), CD4 (conjugated with PE-Cy5; BD Bioscience), CD8a (conjugated with R-PE; BD Bioscience) and CD25 (conjugated with fluorescein isothiocyanate; BD Bioscience) was added to the cells, which were then incubated at 4 °C overnight. Flow-cytometric analysis was performed by using FACS Calibur (BD Bioscience) after washing the cells with PBS. For gating and calculation, CellQuest software (BD Bioscience) was used. In the FACS analysis, 10 000 cells were examined for each sample.

Statistical analysis

Statistical analysis was performed by using GraphPad Prism (GraphPad Software, San Diego, CA, USA). The criterion for statistical significance was $P<0.05$ by Dunnett multiple comparison test.

CONFLICT OF INTEREST

The authors declare no conflict of interest.

ACKNOWLEDGEMENTS

This work was partly supported by Grants-in-Aid for Scientific Research from the Ministry of Education, Culture, Sports, Science and Technology of Japan (nos. 21791664 and 21200022); Science and Culture and Special Coordination Funds for Promoting Science and Technology of the Japanese Government, Strategic Research Programme for Brain Sciences (SRPBS); the Ministry of Health, Labour and Welfare of Japan; and Japan Foundation for Aging and Health and the Programme for Promotion of Fundamental studies in Health Sciences of the National Institute of Biomedical Innovation (NIBIO). I also thank Teru Hiroi for technical support in animal treatment.

1 Hartong DT, Berson EL, Dryja TP. Retinitis pigmentosa. *Lancet* 2006; **368**: 1795–1809.
2 Santos A, Humayun MS, de Juan Jr E, Greenburg RJ, Marsh MJ, Klock IB *et al.* Preservation of the inner retina in retinitis pigmentosa. A morphometric analysis. *Arch Ophthalmol* 1997; **115**: 511–515.
3 Nagel G, Szellas T, Huhn W, Kateriya S, Adeishvili N, Berthold P *et al.* Channelrhodopsin-2, a directly light-gated cation-selective membrane channel. *Proc Natl Acad Sci USA* 2003; **100**: 13940–13945.

4 Bi A, Cui J, Ma YP, Olshevskaya E, Pu M, Dizhoor AM *et al.* Ectopic expression of a microbial-type rhodopsin restores visual responses in mice with photoreceptor degeneration. *Neuron* 2006; **50**: 23–33.
5 Tomita H, Sugano E, Yawo H, Ishizuka T, Isago H, Narikawa S *et al.* Restoration of visual response in aged dystrophic RCS rats using AAV-mediated channelopsin-2 gene transfer. *Invest Ophthalmol Vis Sci* 2007; **48**: 3821–3826.
6 Lagali PS, Balya D, Awatramani GB, Munch TA, Kim DS, Busskamp V *et al.* Light-activated channels targeted to ON bipolar cells restore visual function in retinal degeneration. *Nat Neurosci* 2008; **11**: 667–675.
7 Tomita H, Sugano E, Isago H, Hiroi T, Wang Z, Ohta E *et al.* Channelrhodopsin-2 gene transduced into retinal ganglion cells restores functional vision in genetically blind rats. *Exp Eye Res* 2010; **90**: 429–436.
8 Ishizuka T, Kakuda M, Araki R, Yawo H. Kinetic evaluation of photosensitivity in genetically engineered neurons expressing green algae light-gated channels. *Neurosci Res* 2006; **54**: 85–94.
9 Wang H, Peca J, Matsuzaki M, Matsuzaki K, Noguchi J, Qiu L *et al.* High-speed mapping of synaptic connectivity using photostimulation in Channelrhodopsin-2 transgenic mice. *Proc Natl Acad Sci USA* 2007; **104**: 8143–8148.
10 Tomita H, Sugano E, Fukazawa Y, Isago H, Sugiyama Y, Hiroi T *et al.* Visual properties of transgenic rats harboring the channelrhodopsin-2 gene regulated by the thy-1.2 promoter. *PLoS One* 2009; **4**: e7679.
11 Monville C, Torres E, Thomas E, Scarpini CG, Muhith J, Lewis J *et al.* HSV vector-delivery of GDNF in a rat model of PD: partial efficacy obscured by vector toxicity. *Brain Res* 2004; **1024**: 1–15.
12 Aiuti A, Bachoud-Lévi AC, Blesch A, Brenner MK, Cattaneo F, Chiocca EA *et al.* Progress and prospects: gene therapy clinical trials (part 2). *Gene Therapy* 2007; **14**: 1555–1563.
13 Alexander BL, Ali RR, Alton EW, Bainbridge JW, Braun S, Cheng SH *et al.* Progress and prospects: gene therapy clinical trials (part 1). *Gene Ther* 2007; **14**: 1439–1447.
14 Thomas CE, Ehrhardt A, Kay MA. Progress and problems with the use of viral vectors for gene therapy. *Nat Rev Genet* 2003; **4**: 346–358.
15 Koizumi K, Poulaki V, Doehmen S, Welsandt G, Radetzky S, Lappas A *et al.* Contribution of TNF-α to leukocyte adhesion, vascular leakage, and apoptotic cell death in endotoxin-induced uveitis *in vivo*. *Invest Ophthalmol Vis Sci* 2003; **44**: 2184–2191.
16 Zhang YC, Powers M, Wasserfall C, Brusko T, Song S, Flotte T *et al.* Immunity to adeno-associated virus serotype 2 delivered transgenes imparted by genetic predisposition to autoimmunity. *Gene Therapy* 2004; **11**: 233–240.
17 Damoiseaux JG, Cautain B, Bernard I, Mas M, van Breda Vriesman PJ, Druet P *et al.* A dominant role for the thymus and MHC genes in determining the peripheral CD4/CD8 T cell ratio in the rat. *J Immunol* 1999; **163**: 2983–2989.
18 Kim SA, Lim SS. T lymphocyte subpopulations and interleukin-2, interferon-γ, and interleukin-4 in rat pulpitis experimentally induced by specific bacteria. *J Endod* 2002; **28**: 202–205.
19 Toda A, Piccirillo CA. Development and function of naturally occurring CD4+CD25+ regulatory T cells. *J Leukoc Biol* 2006; **80**: 458–470.
20 Simpson E. A historical perspective on immunological privilege. *Immunol Rev* 2006; **213**: 12–22.
21 Caldwell RB, McLaughlin BJ. Permeability of retinal pigment epithelial cell junctions in the dystrophic rat retina. *Exp Eye Res* 1983; **36**: 415–427.
22 Caldwell RB, McLaughlin RJ, Boykins LG. Intramembrane changes in retinal pigment epithelial cell junctions of the dystrophic rat retina. *Invest Ophthalmol Vis Sci* 1982; **23**: 305–318.
23 Caldwell RB, Wade LA, McLaughlin BJ. A quantitative study of intramembrane changes during cell junctional breakdown in the dystrophic rat retinal pigment epithelium. *Exp Cell Res* 1984; **150**: 104–117.
24 Chang CW, Defoe DM, Caldwell RB. Retinal pigment epithelial cells from dystrophic rats form normal tight junctions *in vitro*. *Invest Ophthalmol Vis Sci* 1997; **38**: 188–195.
25 Nakai H, Yant SR, Storm TA, Fuess S, Meuse L, Kay MA. Extrachromosomal recombinant adeno-associated virus vector genomes are primarily responsible for stable liver transduction *in vivo*. *J Virol* 2001; **75**: 6969–6976.
26 Niemeyer GP, Herzog RW, Mount J, Arruda VR, Tillson DM, Hathcock J *et al.* Long-term correction of inhibitor-prone hemophilia B dogs treated with liver-directed AAV2-mediated factor IX gene therapy. *Blood* 2009; **113**: 797–806.
27 Satofuka S, Ichihara A, Nagai N, Yamashiro K, Koto T, Shinoda H *et al.* Suppression of ocular inflammation in endotoxin-induced uveitis by inhibiting nonproteolytic activation of prorenin. *Invest Ophthalmol Vis Sci* 2006; **47**: 2686–2692.
28 Reichelt W, Dettmer D, Bruckner G, Brust P, Eberhardt W, Reichenbach A. Potassium as a signal for both proliferation and differentiation of rabbit retinal (Muller) glia growing in cell culture. *Cell Signal* 1989; **1**: 187–194.
29 Hartig W, Grosche J, Distler C, Grimm D, el-Hifnawi E, Reichenbach A. Alterations of Muller (glial) cells in dystrophic retinae of RCS rats. *J Neurocytol* 1995; **24**: 507–517.
30 Hao LY, Hao XQ, Li SH, Li XH. Prenatal exposure to lipopolysaccharide results in cognitive deficits in age-increasing offspring rats. *Neuroscience* 2010; **166**: 763–770.
31 Beurel E, Jope RS. Lipopolysaccharide-induced interleukin-6 production is controlled by glycogen synthase kinase-3 and STAT3 in the brain. *J Neuroinflammation* 2009; **6**: 9.
32 Ni YQ, Gan DK, Xu HD, Xu GZ, Da CD. Neuroprotective effect of transcorneal electrical stimulation on light-induced photoreceptor degeneration. *Exp Neurol* 2009; **219**: 439–452.
33 Morimoto T, Miyoshi T, Sawai H, Fujikado T. Optimal parameters of transcorneal electrical stimulation (TES) to be neuroprotective of axotomized RGCs in adult rats. *Exp Eye Res* 2010; **90**: 285–291.
34 Wang J, Jiang S, Kwong JM, Sanchez RN, Sadun AA, Lam TT. Nuclear factor-kappaB p65 and upregulation of interleukin-6 in retinal ischemia/reperfusion injury in rats. *Brain Res* 2006; **1081**: 211–218.
35 Kaltschmidt C, Kaltschmidt B, Neumann H, Wekerle H, Baeuerle PA. Constitutive NF-kappa B activity in neurons. *Mol Cell Biol* 1994; **14**: 3981–3992.
36 O'Neill LA, Kaltschmidt C. NF-kappa B: a crucial transcription factor for glial and neuronal cell function. *Trends Neurosci* 1997; **20**: 252–258.
37 O'Garra A, Vieira P. Regulatory T cells and mechanisms of immune system control. *Nat Med* 2004; **10**: 801–805.
38 Sakaguchi S. Regulatory T cells: key controllers of immunologic self-tolerance. *Cell* 2000; **101**: 455–458.
39 Shevach EM. CD4+ CD25+ suppressor T cells: more questions than answers. *Nat Rev Immunol* 2002; **2**: 389–400.
40 Li W, Asokan A, Wu Z, Van Dyke T, DiPrimio N, Johnson JS *et al.* Engineering and selection of shuffled AAV genomes: a new strategy for producing targeted biological nanoparticles. *Mol Ther* 2008; **16**: 1252–1260.
41 Koga T, Koshiyama Y, Gotoh T, Yonemura N, Hirata A, Tanihara H *et al.* Coinduction of nitric oxide synthase and arginine metabolic enzymes in endotoxin-induced uveitis rats. *Exp Eye Res* 2002; **75**: 659–667.
42 Kügler S, Lingor P, Schöll U, Zolotukhin S, Bähr M. Differential transgene expression in brain cells *in vivo* and *in vitro* from AAV-2 vectors with small transcriptional control units. *Virology* 2003; **311**: 89–95.
43 Auricchio A, Hildinger M, O'Connor E, Gao GP, Wilson JM. Isolation of highly infectious and pure adeno-associated virus type 2 vectors with a single-step gravity-flow column. *Hum Gene Ther* 2001; **12**: 71–76.
44 Auricchio A, O'Connor E, Hildinger M, Wilson JM. A single-step affinity column for purification of serotype-5 based adeno-associated viral vectors. *Mol Ther* 2001; **4**: 372–374.
45 Sugano E, Tomita H, Ishiguro S, Abe T, Tamai M. Establishment of effective methods for transducing genes into iris pigment epithelial cells by using adeno-associated virus type 2. *Invest Ophthalmol Vis Sci* 2005; **46**: 3341–3348.
46 Papathanasiou ES, Peachey NS, Goto Y, Neafsey EJ, Castro AJ, Kartje GL. Visual cortical plasticity following unilateral sensorimotor cortical lesions in the neonatal rat. *Exp Neurol* 2006; **199**: 122–129.
47 Iwamura Y, Fujii Y, Kamei C. The effects of certain H(1)-antagonists on visual evoked potential in rats. *Brain Res Bull* 2003; **61**: 393–398.
48 Boettler T, Spangenberg HC, Neumann-Haefelin C, Panther E, Urbani S, Ferrari C *et al.* T cells with a CD4+CD25+ regulatory phenotype suppress *in vitro* proliferation of virus-specific CD8+ T cells during chronic hepatitis C virus infection. *J Virol* 2005; **79**: 7860–7867.

OPEN ACCESS Freely available online

PLoS one

Dissecting a Role for Melanopsin in Behavioural Light Aversion Reveals a Response Independent of Conventional Photoreception

Ma'ayan Semo[1]*, Carlos Gias[1], Ahmad Ahmado[1], Eriko Sugano[2], Annette E. Allen[3], Jean M. Lawrence[1], Hiroshi Tomita[2], Peter J. Coffey[1], Anthony A. Vugler[1]*

1 Department of Ocular Biology and Therapeutics, University College London-Institute of Ophthalmology, London, United Kingdom, **2** Institute for International Advanced Interdisciplinary Research, Tohoku University, Aoba-ku, Sendai, Japan, **3** Faculty of Life Sciences, University of Manchester, Manchester, United Kingdom

Abstract

Melanopsin photoreception plays a vital role in irradiance detection for non-image forming responses to light. However, little is known about the involvement of melanopsin in emotional processing of luminance. When confronted with a gradient in light, organisms exhibit spatial movements relative to this stimulus. In rodents, behavioural light aversion (BLA) is a well-documented but poorly understood phenomenon during which animals attribute salience to light and remove themselves from it. Here, using genetically modified mice and an open field behavioural paradigm, we investigate the role of melanopsin in BLA. While wildtype (WT), melanopsin knockout (*Opn4*$^{-/-}$) and *rd/rd cl* (melanopsin only (MO)) mice all exhibit BLA, our novel methodology reveals that isolated melanopsin photoreception produces a slow, potentiating response to light. In order to control for the involvement of pupillary constriction in BLA we eliminated this variable with topical atropine application. This manipulation enhanced BLA in WT and MO mice, but most remarkably, revealed light aversion in triple knockout (TKO) mice, lacking three elements deemed essential for conventional photoreception (*Opn4*$^{-/-}$ *Gnat1*$^{-/-}$ *Cnga3*$^{-/-}$). Using a number of complementary strategies, we determined this response to be generated at the level of the retina. Our findings have significant implications for the understanding of how melanopsin signalling may modulate aversive responses to light in mice and humans. In addition, we also reveal a clear potential for light perception in TKO mice.

Citation: Semo M, Gias C, Ahmado A, Sugano E, Allen AE, et al. (2010) Dissecting a Role for Melanopsin in Behavioural Light Aversion Reveals a Response Independent of Conventional Photoreception. PLoS ONE 5(11): e15009. doi:10.1371/journal.pone.0015009

Editor: Steven Barnes, Dalhousie University, Canada

Received August 18, 2010; **Accepted** October 11, 2010; **Published** November 29, 2010

Funding: This work was funded by the London Project to Cure Blindness (www.thelondonproject.org/) and the Lincy Foundation. The funders had no role in study design, data collection and analysis, decision to publish, or preparation of the manuscript.

Competing Interests: The authors have declared that no competing interests exist.

* E-mail: a.vugler@ucl.ac.uk (AAV); m.semo@ucl.ac.uk (MS)

Introduction

In the 1920's, Crozier and Pincus showed that neonatal rats with closed eyelids will move away from bright light along a gradient towards a less intensely illuminated target [1]. Adult rats retain an aversion to light [2,3], so strong that it can be used as a motivating factor in behavioural learning paradigms [4]. Like rats, adult mice also show behavioural light aversion (BLA) to acute (10–30 mins) light exposure in the open field [5,6]. Using mice, the "light/dark box test" has been employed extensively in drug development to identify putative anxiolytic compounds (see [5], reviewed in [7]) and more recently to investigate human photophobia in mouse models of migraine [8,9]. Despite the widespread application of this behavioural phenomenon, and its undoubted importance to the lives of nocturnal animals, little is known about the neural circuitry mediating BLA in rodents. Although one study to date has implicated both subcortical and cortical processing [10], the contribution of different photoreceptive components from the retina remains unclear.

In the mammalian retina, rods/cones of the outer retina are known to mediate image-forming vision [11,12], while photoreceptive melanopsin-expressing retinal ganglion cells (mRGCs) of the inner retina sub serve most non-image-forming responses to light [13,14,15,16,17]. If the eyes are enucleated bilaterally, then BLA in rats is abolished [10]. To date, only a few studies shed light on the important question of whether melanopsin alone could mediate this primitive non-image-forming response. These studies, from a variety of animal models, report mixed conclusions about a potential role for melanopsin in BLA.

A recent study investigating the role of melanopsin in non-image forming functions found that targeted destruction of melanopsin cells had no impact on the light:dark preference of mice [18]. This is in line with data from RCS rats showing a progressive loss of BLA over time, with no response detectable by 7 months [19]. Another study using *rd* mice also failed to report a significant light aversion response following exposure to illumination of 2800 Lux [20].

In contrast, spatial responses to light have been reported in *rd* mice given the choice between light and dark living/nesting areas over a 22 h period [21]. Here, retinal degenerate mice spent significantly more time in the dark than the illuminated area, a response that could be eliminated by enucleation. However, as *rd* mice retain a significant population of remodelled cones with identifiable presynaptic stuctures [22,23,24,25] they are unsatisfac-